5-2018

Targeting Mitochondrial Proline Dehydrogenase (PRODH) with a Suicide Inhibitor as a Novel Anticancer Strategy

Beatrice Becker
Dominican University of California

https://doi.org/10.33015/dominican.edu/2018.bio.05

Targeting Mitochondrial Proline Dehydrogenase (PRODH) with a Suicide Inhibitor as a Novel Anticancer Strategy

By

Beatrice Cortina Becker

A culminating thesis submitted to the faculty of Dominican University of California in partial fulfillment of the requirements for the degree of Master of Science in Biology

San Rafael, California

May, 2018

This thesis, written under the direction of candidate's thesis advisor and approved by the thesis committee and the MS Biology program director, has been presented and accepted by the Department of Natural Sciences and Mathematics in partial fulfillment of the requirements for the degree of Master of Science in Biology at Dominican University of California. The written content presented in this work represents the work of the candidate alone.

Beatrice Cortina Becker

Candidate 05 / 11 / 2018

Dr. Christopher Benz

Thesis Advisor 05 / 11 / 2018

Dr. Ekaterina Kalashnikova

Second Reader 05 / 11 / 2018

Dr. Meredith Protas

Program Director 05 / 11 / 2018

Table of Contents

List of Tables

List of Figures

Figure 6	PPG treatment of ZR-75-1 cells (24-72h). The PRODH suicide inhibitor, PPG, following its rapid inhibition of PRODH enzyme activity induces a time-dependent selective degradation of PRODH protein (30-60%) within 24 to 72 hours of cell culture treatment. Mitochondrial complex-1 protein NDUFS1 slightly declines over time, but the cytoplasmic FAD containing protein MTHFR does not, and tracks with total cell actin levels.
Figure 7	Mitochondrial PRODH lost within 24h of PPG without mitochondrial destruction. PPG treatment induces early loss of mitochondrial PRODH protein before loss of outer mitochondrial membrane or later cell death. Top panel untreated ZR-75-1 cells stained for PRODH (red) and mitochondrial TOM20 (green). Bottom panel identical to top panel but cells treated with 5mM PPG for 24 hours.
Figure 8	Cytosolic MTHFR (FAD-containing) protein not affected by PPG validates western blot data. Top panel untreated ZR-75-1 cells stained for cytosolic MTHFR (red) and PRODH (green). Bottom panel identical to top panel but cells treated with 5mM PPG for 24 hours
Figure 9A	E3 ligase PARKIN not affected by PPG validates the absence of mitophagy. Top panel untreated ZR-75-1 cells stained for PARKIN (red) and mitochondrial TOM20 (green). Bottom panel identical to top panel but cells treated with 5mM PPG for 24 hours.
Figure 9B	Live Cell Imaging of ZR-75-1 cells. Healthy mitochondria (green) detected after 24 hour treatment of 5-oxo and PPG using MitoTracker intercalating dye, a mitochondria marker. Comparable mitochondria marked in green punctate by MitoTracker shows no changes between treatments relative to control.
Figure 9C	Laser confocal images of ZR-75-1 cells upon 24h PPG treatment displays PRODH (green) intensity diminished. Compressed Z stack on confocal microscope of ZR-75-1 cells showing PRODH (green) intensity diminished on cells treated with 5mM PPG for 24 hours
Figure 9D	Western analysis of ZR-75-1 cells treated with 24h 5mM PPG vs. 24h 5mM 5-oxo compared to vehicle control for their PRODH protein levels (67kD) normalized to β-actin (~40kD). Western data confirms 5-oxo has no significant impact upon PRODH levels; while PPG treatment produces significant reduction in PRODH levels, 5-oxo only slightly reduces PRODH levels.
Figure 10	GRP75 communication with TOM20 in mitochondria is disrupted after 24h PPG. Top panel untreated ZR-75-1 cells stained for GRP75 (red) and mitochondrial TOM20 (green). Bottom panel identical to top panel but cells treated with 5mM PPG for 24 hours.

Abstract

Proline dehydrogenase (PRODH) is a p53-inducible inner mitochondrial membrane protein linked to electron transport and capable of generating mitochondrial glutamate and intracellular ATP, especially under cellular stress conditions. Among a panel of 51 human breast cancer cell lines, PRODH and glutaminase (GLS1) expression levels were found to be inversely correlated (1) implicating two independent and alternative mitochondrial pathways supplying anaplerotic glutamate for cancer cell energy production and macromolecular synthesis. Proposing PRODH to be a promising cancer therapeutic target, we compared the *in vitro* cellular effects of PRODH knockdown by siRNA as well as competitive (L-tetrahydrofuroic acid, THFA; or 5-oxo-2-tetrahydrofurancarboxylic acid, 5-oxo) and irreversible/suicide (PPG) inhibitors of PRODH using cultured human breast cancer cells. PRODH knockdown or enzymatic inhibition each inhibited cell growth and induced variable degrees of apoptosis against malignant breast epithelial cell lines (ZR-75-1, DU4475, MCF-7) without affecting immortalized and non-malignant breast epithelial cells (MCF-10A). Loss of PRODH function produced additive *in vitro* anticancer effects when combined with either a p53 upregulator (MI-63) or a glutaminase inhibitor (CB-839) (2). Unlike the competitive inhibitors, PPG not only demonstrated irreversible inhibition of PRODH enzymatic activity on isolated breast cancer cell mitochondria (ZR-75-1) but it also induced loss of mitochondrial PRODH expression prior to its induction of cancer cell apoptosis. Computer modeling of PRODH's enzymatic pocket occupied by either 5-oxo or PPG revealed that PPG likely induces molecular distortion, suggesting its unique ability to activate apoptosis by first triggering mitochondrial stress; however, it remains unclear

whether the cancer cell's ultimate response to this initial mitochondrial stress is mediated by mitophagy or by the mitochondrial unfolded protein response (UPR^{mt}). The two objectives of this current project address both the mechanistic questions about mitochondrial stress induced by the suicide PRODH inhibitor, PPG, as well as a more translational question about the *in vivo* feasibility of systemically administering PPG as a potential therapeutic. To address the first objective, we employed confocal intracellular imaging to investigate the mitochondrial stress induced by PPG. To address the second objective, PPG was administered *in vivo* to flies and mice (implanted with xenografted human breast tumors) to observe both whole organism and tissue-specific effects of this mitochondrial stress inducing suicide inhibitor of PRODH. These studies form the basis for more extended *in vivo* preclinical testing of PRODH suicide inhibitors as a potential new breast cancer treatment strategy.

Introduction

Breast cancer classification

Breast cancer is currently classified clinically and molecularly by the presence or absence of overexpression of three different breast cancer biomarkers: estrogen receptor-α (ER), progesterone receptor (PR), and human epidermal growth factor receptor-2 (HER2 or ERBB2) (3, 4, 5). In conjunction with their expression, these three biomarkers define four primary intrinsic subclasses of breast cancer: luminal A (ER+ and/or PR+, HER2-), luminal B (ER+ and/or PR+, HER2+), HER2-enriched (ER- and PR-, HER2+) and basal-like (ER-, PR- and HER2-; sometimes referred to as "triple-negative") breast cancers (6, 7). Each of these four biological subclasses of breast cancer is clinically distinct with respect to both patient prognosis and treatment approaches. These subtypes have been investigated at the molecular level in order to find specialized interventions to combat breast cancer tumors that do not respond to treatments or relapse. No single therapy works one hundred percent of the time and that is why multiple therapeutic strategies are being evaluated in an attempt to produce efficient intervention for tumors regardless of their molecular subtype. The search continues for new targeted therapies as the field unravels what aspects could be uniform for different types of tumors and not necessarily a very specific molecular subtype.

Breast cancer metabolic reprogramming with dependence on GLS1 or PRODH for mitochondrial glutamate production

Other than the established biomarkers, there is a great need to identify novel biomarkers and new drug targets that will potentially improve the clinical outcome of breast cancer patients. Bioenergetics and mitochondrial function studies can help answer

the question where cancers get their energy from, while manipulating energetics would be beneficial for many tumor types, for some of them this could even be a unique treatment. There has been a growing appreciation of cancer cell metabolic reprogramming as a driving force underlying the biology of many different types of cancers, including breast cancer (8, 9). Known for over a half century, the Warburg effect first pointed out that cancer cells commonly generate energy mostly via cytosolic glycolysis, even under aerobic conditions, rather than by mitochondrial pyruvate oxidation (10).

The replication and growth of cancer cells depends heavily on energetics and mitochondrial glutamate production for both cell energy levels and biosynthetic reactions; glutamate may be generated by either glutaminase (GLS1) or proline dehydrogenase (PRODH) enzymes as their overexpression appears to be inversely correlated across different human breast cancer cell lines (Fig. 1) (1). Glutaminase is a mitochondrial enzyme transcriptionally upregulated by the oncogene c-MYC, and it converts glutamine into glutamate for anapleurosis and ATP production (11). The importance of c-Myc induced GLS1 overexpression in generating cancer cell "glutamine addiction" has been well recognized for nearly a decade. In contrast, less appreciated in this regard is the critical role of p53wt induced PRODH, the 67 kDa enzyme found within the inner mitochondrial membrane (12) that catalyzes the first and most rate-limiting step in proline oxidation, a process that in two metabolic steps subsequently leads to mitochondrial glutamate production (13). PRODH's enzymatic product is the unstable intermediate P5C, pyrroline-5-carboxylate, releasing two electrons that are immediately transferred into the mitochondria's electron transport chain where they can be used for

either ATP production or ROS generation (Fig. 2) (1). If these electrons are optimally transported, each molecule of catabolized proline can yield up to 30 ATP molecules (14), and further oxidation of P5C by P5CDH yields mitochondrial glutamate (Fig. 2).

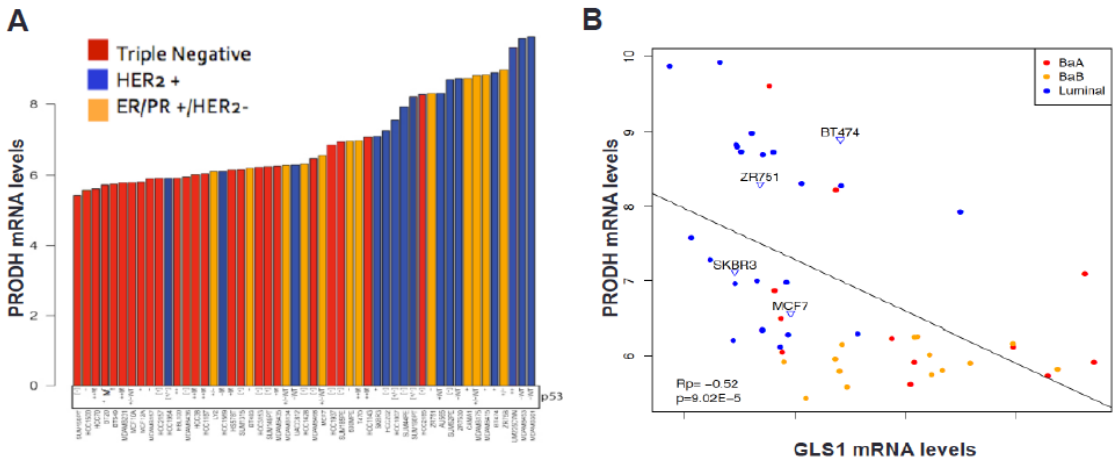

Figure 1. (A) PRODH mRNA expression levels (normalized, log2-scaled) across 51 different human breast cancer cell lines determined from published microarrays (15) and color coded by intrinsic subtype, highest in luminal and lowest in triple-negative breast cancers (1). (B) PRODH and GLS1 mRNA levels strongly inversely correlated; indicated models are among those being evaluated for combination therapy (1).

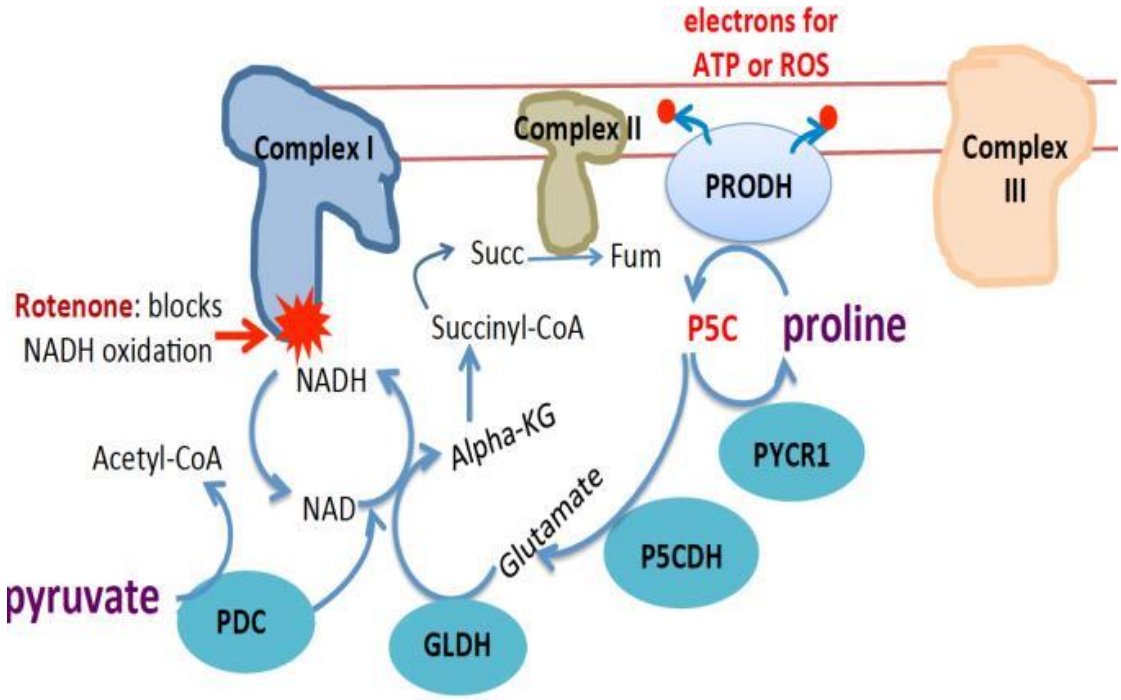

Figure 2. Induced by p53, mitochondrial PRODH catalyzes the first step of proline oxidation to produce the unstable metabolic intermediate, P5C, with two electrons transferred into the electron transport chain for either ATP production or ROS generation, and downstream mitochondrial reactions generating glutamate, α-KG, and NADH. Pyruvate oxidation by PDC produces acetyl Co-A and also increases the NADH pool. Rotenone blocks all Complex 1 oxidation of NADH to NAD (1).

In naturally occurring organisms, the *in vivo* use of proline dehydrogenase (PRODH) has long been known to be critical for energy production in flies (*Drosophila melanogaster*) and more recently, for stress resistance in worms (16). PRODH was first identified in mammals as PIG-6 (p53 inducible gene-6) by Polyak *et al* (17) and its mitochondrial localization was noted during the study of the *in vivo* importance of proline derived from the breakdown of extracellular matrix collagen to sustain Krebs cycle generation of ATP (18, 19). Early on, Phang *et al.* proposed that PRODH served as a tumor suppressing mediator of p53wt activity, inhibiting tumor growth by producing ROS and inducing apoptosis (8, 10, 11). Subsequent studies called this conclusion into question by documenting PRODH's ability to promote cancer cell survival via

anaplerotic glutamate production and mitochondrial ATP production, especially under nutrient and oxygen stress conditions (9, 11, 20). Presently, it is thought that proline oxidation by PRODH generates either mitochondrial ATP or ROS production, depending on the integrity of the electron transport chain, but not as a direct product of PRODH enzymatic activity (21). Using human luminal breast cancer cell line models, Benz laboratory studies add compelling support to the hypothesis that proline oxidation primarily produces ATP as an essential cell survival mechanism (22).

Tumor suppressor p53, its transcriptional control of PRODH and their regulation by MDM2

Cellular expression of PRODH is predominantly regulated by the transcription factor p53, a model first shown when the identity of PRODH was not clear and it was referred to as PIG-6 (17). Well established at the time was the fact that p53 is a tumor suppressor protein, often referred to as the "guardian of the genome," serving to coordinate cellular responses to genome injury by inducing either cell cycle arrest (cytostasis), enabling DNA damage to be repaired, or programmed cell death (apoptosis) when DNA damage is too severe to be repaired. In response to DNA damage, p53 protein levels are upregulated and transcriptionally induce other DNA damage response genes and cell cycle regulating genes including the cyclin dependent kinase 1 (CDK1) inhibitor and p21 that together initiate cell cycle arrest (21), allowing other genes to assess the extent of genome damage and thereby determine the cell's ultimate fate: apoptosis versus cytostasis. If the DNA damage can be repaired, p53 also activates the necessary repair mechanisms; but if DNA damage cannot be repaired, p53 further signals the cell to undergo apoptosis, preventing the damaged DNA to be passed onto the next generation.

The cellular decision between cytostasis and apoptosis following activation of the

p53 pathway has important implications for tumor progression and therapy. In many cancer cells, where p53 is mutated, their ability to transcriptionally regulate cell fate is lost, allowing those cancer cells to continue dividing and surviving in the face of genomic damage, in fact, further facilitating their development of additional oncogenic mutations (23). In other cancer cells, including most luminal and HER2+ breast cancers, p53 is not mutationally inactivated but rather its level of protein expression is often kept suppressed by the overexpression of MDM2, an E3 ubiquitin-protein ligase that causes the constitutive proteosomal degradation of p53 (21, 23). It has been observed in human cell line models of luminal and HER2+ subtypes specifically, that these express higher transcript levels of PRODH and wildtype p53 tumor suppressor gene (p53wt), while triple-negative breast cancers most frequently express mutated versions of p53 (p53mut).

Largely because of the frequent incidence of luminal breast cancer, approximately 75% of breast cancers overall express wildtype p53 protein (p53wt) (23, 24) and do not express any mutated p53 (p53mut) (Table 1) (24). In such ER+ breast cancers, the frequency of p53mut can be as low as 10%, while HER2+ breast cancers have a higher p53mut frequency that can reach 40%; in contrast, triple-negative breast cancers have a p53mut frequency exceeding 70% (24). Currently studied by the Benz group, the endogenous level of expression of p53wt can be upregulated by 5-10 fold following treatment with a p53 restoring drug such as an MDM2 inhibitor (e.g. Nutlin or MI-63) in both normal and malignant cells (25). As a result, this p53wt induction by an MDM2 inhibitor also increases the expression of various p53 inducible genes such as p21 and PRODH, causing changes in mitochondrial bioenergetics and triggering either cytostasis (in normal cells) or apoptosis (in cancer cells) (1).

Triple-negative breast cancers that express p53mut are not sensitive to an MDM2 inhibitor; rather, they are frequently associated with c-Myc oncogene overexpression which transcriptionally induces glutaminase (GLS1) expression, causing these breast cancers to be glutamine-addicted by which much of their tumor cell energy comes from mitochondrial glutamate production (Fig. 2), rendering them therapeutically susceptible to another inhibitor studied by the Benz group, a glutaminase (GLS1) inhibitor like Calithera's CB-839 (1). While luminal breast cancer cells that express p53wt but lack c-Myc overexpression are similarly dependent on mitochondrial glutamate production for energy and synthetic reactions, their glutamate production comes from p53wt induced PRODH and not from GLS1 overexpression. These differences help explain the inverse relationship observed between GLS1 and PRODH transcript expression observed across luminal vs triple-negative breast cancer cell line models (Fig. 1). These differences also suggest that, regardless of the breast cancer subtype, simultaneously inhibiting both PRODH and GLS1 pathways might result in a more complete suppression of mitochondrial glutamate levels and therefore serve as a more effective and general breast cancer treatment strategy than therapeutically inhibiting either pathway alone.

Table 1. Frequency of wildtype p53 (p53wt) versus mutated p53 (p53mut) found in ER-positive (ERpos) and ER-negative (ERneg) subsets of early-onset and late-onset breast cancers (24).

Table 1

***n* = 289**	**ERneg/p53wt (%)**	**ERpos/p53wt (%)**	**ERneg/p53mut (%)**	**ERpos/p53mut (%)**
Late-onset (≥70 years), *n* = 154	25 (16.2%)	107 (69.5%)	12 (7.8%)	10 (6.5%)
Early-onset (≤45 years), *n* = 135	49 (36.3%)	64 (47.4%)	14 (10.4%)	8 (5.9%)

p = 0.0004, Fisher Exact.

Cancer cell responses to PRODH protein manipulations

Energetics is really important for cancer cells and several manipulations have been attempted in order to prevent proline catabolism to limit both mitochondrial glutamate and ATP production in such cancer cells. In targeting proline catabolism as a potential cancer therapeutic, the Benz group has studied different approaches including genetically knocking down PRODH and P5CDH enzymes, and blocking PRODH's enzymatic activity with competitive and suicide inhibitors, all focusing to reduce breast cancer cell growth and viability.

Addressing the strategic question of whether to target PRODH or the next enzymatic target involved in mitochondrial proline catabolism and glutamate production, P5CDH, Benz group investigators knocked down P5CDH and evaluated the knockdown effect on cell viability in combination with MI-63 treatment, and observed less c-PARP production (PARP cleavage, reflecting apoptosis) when compared to PRODH knockdown combined with MI-63; suggesting that targeting PRODH would lead to

greater antitumor activity than targeting a different mitochondrial enzyme in the same proline catabolic pathway (1, 25). Results of PRODH knockdown by siRNA have shown enhanced apoptosis in human breast cancer cells lines of low (MCF-7) and high (ZR-75-1) PRODH transcript levels, respectively (Fig. 3A). Increased levels of apoptosis occurred in MCF-7 and DU4475 (characterized by their very low PRODH expression) breast cancer cells when PRODH knockdown was combined with 24-48 hours of MI-63 treatment (Fig. 3B-3C). These results show that PRODH knockdown combined with the upregulation of p53 (MI-63 treatment) produces a 4-fold greater capacity to eradicate breast cancer cells compared to MI-63 treatment alone.

The current focus of the Benz laboratory became a comparison of luminal breast cancer cell responses when treated with either competitive or suicide PRODH inhibitors (26). In order to investigate the mechanistic rationale for focusing on an irreversible/suicide PRODH inhibitor rather than a competitive PRODH inhibitor, Benz group medicinal chemistry collaborators first produced a human PRODH structural model for drug discovery and design purposes, where primitive bacterial amino acids were replaced with human ones (2). Tanner *et al.* first crystalized bacterial PRODH in the oxidized state containing FAD along with the competitive proline analog, L-tetrahydrofuroic acid (L-THFA) (27); no mammalian or human PRODH structure was available before or has since become available. Studies were performed by inhibiting the human PRODH structural model with L-THFA, another competitive inhibitor, 5-oxo-2-tetrahydrofurancarboxylic acid (5-oxo) and the newly synthesized and patented inhibitor N-propargylglycine (PPG) (26). Greater hydrogen-bond affinity to PRODH's catalytic site was observed with the newer competitive inhibitor, 5-oxo, relative to a model bound

to the previously described proline analog, L-THFA (27). However, the difference between reversible and irreversible PRODH inhibitors (5-oxo vs. pre- and post-reactive states of PPG) is that the catalytic pocket bound with 5-oxo is structurally undistorted, whereas the post-reactive pocket where PPG is covalently linked to the FAD moiety is structurally distorted (Fig. 4).

Numerous assessments of these PRODH inhibitors have been investigated and the facts are suggestive of PPG being a more interesting and superior inhibitor to target proline catabolism than competitive inhibitors. First, mitochondria from ZR-75-1 cells that were treated with 5-oxo exhibit the same production of NADH as cells treated with PPG, when given the substrate proline to metabolize. However, the reversible competitive inhibitor 5-oxo is washed away when mitochondria are rinsed losing the inhibitory effect while the irreversible inhibitor PPG remains bound (Fig. 5), inhibiting proline metabolism. Secondly, PRODH inhibition creates a synthetic lethal therapeutic opportunity by combining PPG with either an MDM2 inhibitor or a glutaminase inhibitor (1, 2, 25) owing to the ability of the competitive inhibitor L-THFA to act in a similar synthetic lethal interaction with an MDM2 inhibitor and capable to significantly reduce *in vitro* growth (% viability) of DU4475 cells compared to either treatment administered alone (Fig. 3D). Thirdly, supplementary data demonstrate the ability of the suicide inhibitor PPG to promote PRODH degradation in ZR-75-1 cells days before any changes in mitochondrial complex-1 protein, NDUFS1 could be detected; and in the absence of any degradation occurring in an extra-mitochondrial FAD-containing enzyme, methylenetetrahydrofolate reductase (MTHFR) (Fig. 6). This selective degradation of mitochondrial PRODH is only seen in cells treated with PPG, and was not observed after

treatment with competitive inhibitors given at a dose able to fully inhibit PRODH enzymatic activity. Lastly, it has been observed that non-malignant epithelial cells (MCF-10A) do not appear to be susceptible to the growth inhibiting consequences of PRODH inhibition, raising the provocative suggestion that normal cells within an organism treated *in vivo* with a PRODH suicide inhibitor might actually benefit via mitohormesis, an organismal response to sublethal mitochondrial stress, capable of activating cytosolic signaling pathways and ultimately nuclear gene expression (28) enhancing cell stress resistance and improving healthspan.

Two different but plausible cellular responses to any type of mitochondrial stress are mitochondrial unfolded protein response (UPR^{mt}) and mitophagy, the degradation of mitochondria by autophagy. The induction of mitochondrial PRODH decay observed with PPG treatment, and not observed following either L-THFA or 5-oxo treatments, understandably has consequences to the mitochondria. UPR^{mt} is a conserved cellular stress response initiated by loss of protein homeostasis (proteostasis) induced by mis-/unfolded proteins within the mitochondria and followed by a specific pattern of intracellular cell signaling and transcription that includes induction of mitochondria-specific chaperones (29). UPR^{mt} promotes stabilization and recovery of stressed mitochondria while mitophagy serves to remove the most severely damaged of these essential organelles. Often beginning with the same initiating response to stress, such as loss of mitochondrial protein import and outer membrane accumulation of the ubiquitin ligase PARKIN, a cell's net accumulation and severity of stressed mitochondria appears to determine whether either UPR^{mt} or mitophagy will ensue. These alternate mitochondrial fates are difficult to predict but are later associated with different cell

signals and pathways, and can subsequently be distinguished by determining whether there is mitochondrial loss preceded by the selective degradation of a mitochondrial protein like PRODH.

Unfolded protein response is a difficult mechanism to prove definitively due to the lack of absolute molecular criteria that can identify the mechanism in progress, as there are no set of consensus criteria and reagents currently available to definitively prove or disprove that UPR^{mt} is occurring, apart from the alternative mitochondrial consequence, mitophagy. Yet, the induction of the corrective mitochondrial chaperone HSP60 appears to be one specific cellular manifestation of the UPR^{mt} (2, 26). As a chaperone protein, HSP60 surveils cells and their environment in search of misfolded or unfolded proteins, and literature review indicates that HSP60 gets induced as a part of the early set of steps triggering the UPR^{mt}. Currently, the primary evidence that UPR^{mt} occurs in response to PPG treatment is that mitochondrial PRODH decay takes place within 120 minutes of the PPG treatment and in the absence of ensuing mitochondrial destruction or the extra-mitochondrial decay of other FAD-containing enzymes (Fig. 6). In this ability to induce UPR^{mt}, PPG appears to be a superior anticancer candidate relative to competitive PRODH inhibitors, L-THFA and 5-oxo that do not induce the same target enzyme decay, which is expected to permanently minimize the cancer cell's ability to generate ATP and glutamate for growth, replication and metastatic spread (1). Thus, a cancer cell's dependence on glutamine and anaplerotic ATP production provides support for the preclinical development of PRODH suicide inhibitors such as PPG.

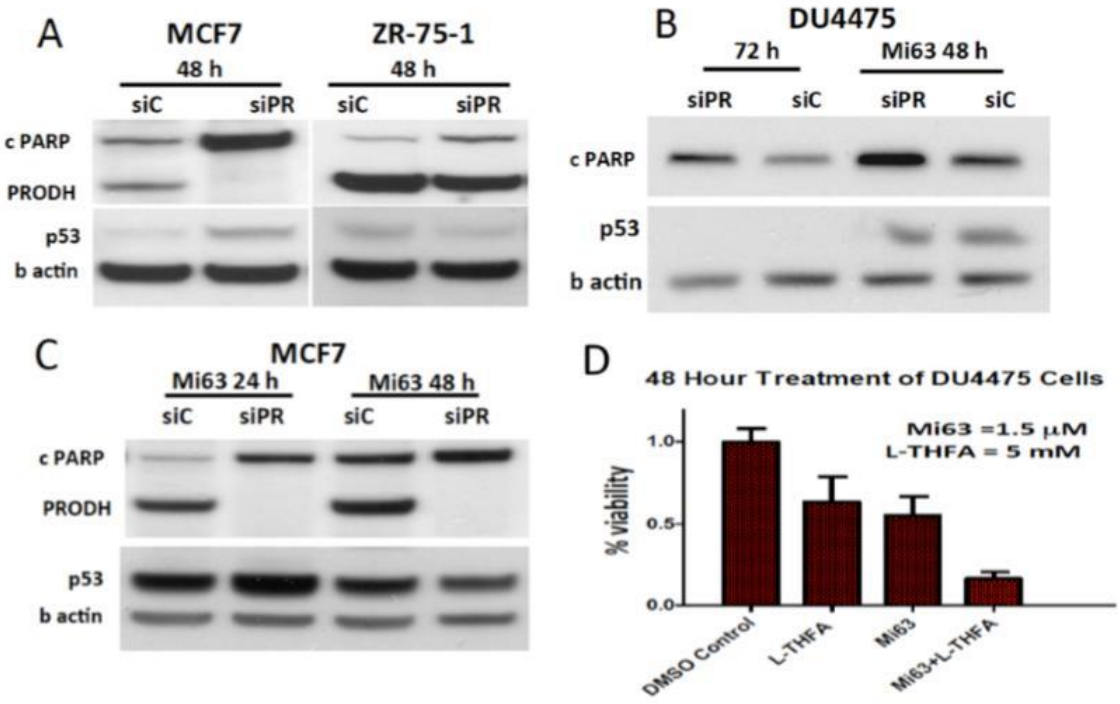

Figure 3. (A) PRODH siRNA knockdown (siPR) in MCF7, ZR-75 and (B) DU4475 breast cancer cells induce apoptosis detected by cleaved (c) PARP on Western blots, less so in ZR-75-1 cells whose higher PRODH levels are more difficult to reduce by siRNA knockdown (A). When combined with MI-63 (24-48 h) restoration of p53wt, PRODH knockdown in the DU4475 (B) and MCF7 (C) cells produces synthetic lethality with marked increase in apoptosis (c PARP). (D) Viability assay demonstrates synthetic lethality effectiveness of L-THFA combined with MI-63 in DU4475 (1). Figures presented at AACR annual meeting poster presentation (2), unpublished data.

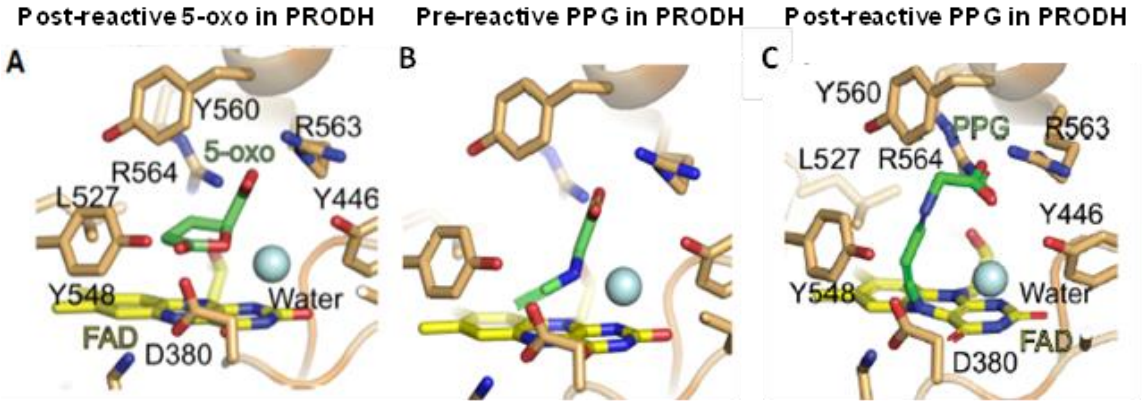

Figure 4. Model of human PRODH's catalytic site containing the tyrosine (Y548) and arginine (R564, R563) hydrogen-bonded to (A) PRODH competitive inhibitor, (S)-(+)-5-oxo-2tetrahydrofurancarboxylic acid (5-oxo, green). The FAD moiety and intercalated water molecule are shown in yellow and blue, respectively. PRODH bound to both pre- (B) and post-reactive (C) N-propargylglycine structure (PPG, green) covalently bound with FAD and showing pocket distortion (1). Figure presented at 2015 & 2017 AACR annual meetings (2, 22).

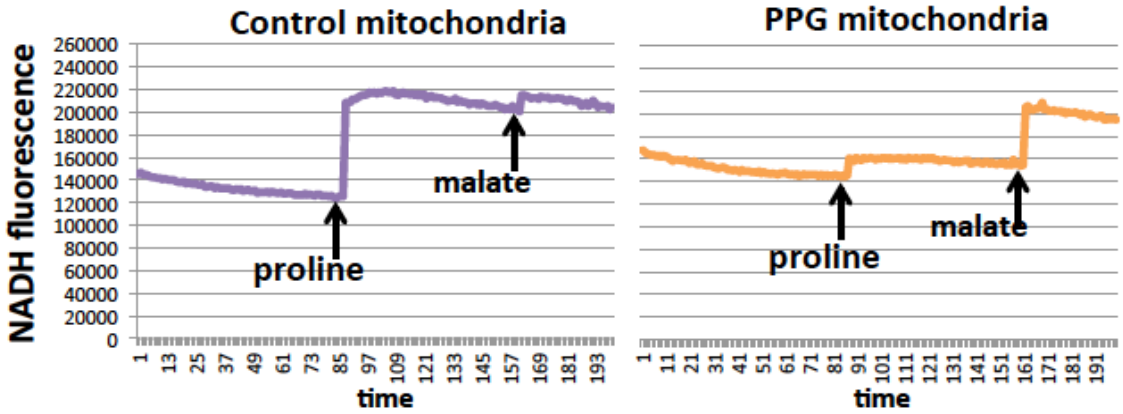

Figure 5. Mitochondria isolated from PPG pretreated (15 h) & washed (30 min) ZR-75-1 cells cannot metabolize proline, although malate metabolism remains unaffected; 5-oxo inhibition is lost by wash out (not shown). 1mM Proline added first, followed by 1mM malate (1). Figure presented at 2017 AACR annual meeting (22).

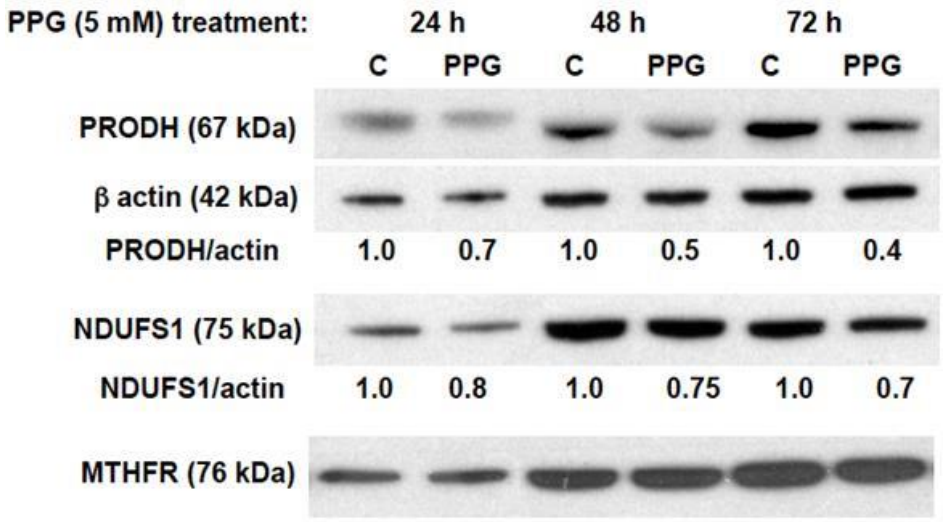

Figure 6. PPG treatment of ZR-75-1 cells (24-72h). The PRODH suicide inhibitor, PPG, following its rapid inhibition of PRODH enzyme activity induces a time-dependent selective degradation of PRODH protein (30-60%) within 24 to 72 hours of ZR-75-1 culture treatment. Mitochondrial complex-1 protein NDUFS1 slightly declines over time, but the cytoplasmic FAD containing protein MTHFR does not, and tracks with total cell actin levels (1). Figure presented at 2017 AACR annual meeting (22).

Addressing the question of whether administering *in vivo* a suicide inhibitor like PPG, at a dose sufficient to inhibit PRODH and induce its mitochondrial decay, is at all feasible and capable of being tolerated in an intact organism, collaboration between the Benz and Jasper laboratories at the Buck Institute for Research on Aging generated data in *Drosophila melanogaster* shown in the attached video. Since flies use proline metabolism to power their flight muscles (16), flies with genetic knockout of PRODH are viable but unable to fly, displaying the "*Sluggish-A*" phenotype. After 48 hours of PPG intake (administered orally as 5mM in sucrose solution), treated flies mimic the "*Sluggish-A*" phenotype (right tube) with reduced flight but without any observed loss of viability or fertility. On the other hand, control flies (fed sucrose with DMSO vehicle but without PPG) showed normal flight activity and health identical to that of wild type flies (left tube). The applied and widely used fly climbing assay is a well-accepted measure of

health; especially in assessing neuronal and muscular decline (30). This *in vivo* fly response and *Sluggish-A* phenotype produced within 48 hours of PPG administration supports the conclusion that in flies, PPG can be ingested orally at a bioavailable dose enabling drug transit to a distant organismal site (e.g. wings and flight muscles) and achieving *in vivo* concentration sufficient to produce a prolonged and significant loss of cellular PRODH enzymatic activity (e.g. need for cellular flight muscle function).

These fly studies formed the basis for further investigation if PPG can similarly be administered *in vivo* at a bioavailable dose that will be tolerated by mammals (such as mice). Since this project's inception, other investigators have recently begun considering PRODH inhibition as a potential cancer treatment strategy. Very recently, Elia *et al* examined the effect of using a competitive PRODH inhibitor (L-THFA) on either 2D (monolayer) or 3D (spheroid) growing cancer cells *in vitro*, reasoning that 3D cell growth might be a better *in vitro* simulation of *in vivo* cancer metastasis (31). These investigators demonstrated that the relative hypoxia and nutrient deficiency of cancer cells growing in 3D spheroids actually produced 3-fold more cellular PRODH compared to the same cancer cell growing in 2D monolayers, again supporting the need to consider conducting experiments employing PRODH inhibitors *in vivo* where the stress conditions of cancer cell growth are likely more severe than those present under standard *in vitro*

cancer cell growth conditions, and where cancer cell dependence on PRODH enzymatic activity may be much greater.

Moving beyond this most recent work from other investigators, we hoped to demonstrate that a PRODH inhibitor like PPG when administered *in vivo* could be tolerated by mammals at a bioavailable dose that would also produce mitochondrial decay of PRODH in an organ system or implanted tumor. The focus of this study on PRODH, whose expression and enzymatic activity is mitochondrially localized, is not necessarily restricted to any specific breast cancer subtype, or even breast cancer vs. other types of epithelial malignancies. In general, the link between cancer and mitochondrial function is that mitochondrial glutamate produced by proline dehydrogenase powers cancer cells, therefore targeting mitochondrial energetics in glutamate-addicted cancer cells produces a powerful approach to combat luminal breast cancer. Inhibiting PRODH alone only temporarily targets proline catabolism whereas inhibiting PRODH with a suicide inhibitor like PPG achieves a higher level of commitment where PRODH is essentially eradicated hindering its ability to generate ATP and mitochondrial glutamate. All the preliminary data at this point suggest PRODH protein levels can be targeted molecularly in order to lessen the energy used to fuel glutamate-addicted cancer cells.

Methods & Materials

❖ Reagents/antibodies/drugs and PPG synthesis

The immunoblotting antibody anti-PARP/cPARP (46D11) rabbit monoclonal was purchased from Cell Signaling (Danvers, MA). ERα mouse monoclonal (clone F-10), rabbit polyclonal and β-actin mouse monoclonal (C4) antibodies were purchased from Santa Cruz Biotechnology (Santa Cruz, CA). The goat anti-mouse secondary HRP-conjugated antibody was purchased from Bio-Rad Laboratories, Inc. (Hercules, CA); the α-tubulin mouse monoclonal antibody (T9026) and 5-oxo-2-tetrahydro-furancarboxylic acid (5-oxo proline dehydrogenase inhibitor) from MilliporeSigma (St. Louis, MO). The following were purchased from Santa Cruz Biotechnology: mouse monoclonal PRODH antibody (A-11); mitochondrial mouse monoclonal NDUFS1 (E-8); mitochondrial mouse monoclonal Rieske FeS IgG (A-5). The NDUFS1 Rabbit Polyclonal Antibody was purchased from ProteinTech^{TM} (Rosemont, IL). The Alexa 488 goat anti-mouse and Alexa 594 goat anti-rabbit secondary antibodies were purchased from Life Technologies (Thermo Fisher Scientific, Carlsbad, CA). The mouse anti ATP-synthase α and mouse anti-cytochrome C were purchased from BD Biosciences Transduction Labs (San Jose, CA).

PPG was synthesized in two-day process: 5ml of DEPC water mixed with 5 grams of propargylamine (MilliporeSigma) over 5 ml of cold water plus the slow addition of 2 grams of iodoacetic acid (stored at -20^{o}C) before overnight incubation at room temperature. Thermo Fisher Scientific™ Savant™ SPD131DDA SpeedVac™ Concentrator was used to dry down volume and sample was divided into Eppendorf tubes to dry on SpeedVac. Samples were pooled together and 2.5mL of ethanol was added,

followed by 30.5mL of acetone and 3.25mL of ethanol. The resulting precipitate was dried and washed extensively using a Buchner funnel. The dried powder was validated by HPLC-mass spectrometry and NMR by our collaborator Dr. Bryan Cowen at the University of Denver, Denver, Colorado.

- **Cell Culture Growth, Treatment and Harvest of Human Breast Cancer Cell Lines**

MCF-7 and ZR-75-1 human breast cancer cell lines were purchased from ATCC (American Type Culture Collection, Manassas, VA) and grown in RPMI medium supplemented with 10% fetal bovine serum (Cellgro, Manassas, VA). Experimental cells were treated with 5mM N-propargylglycine in RPMI medium supplemented with 10% fetal bovine serum for 12, 24, 48, 72, or 96 hours. Optimal concentration determined in the previous dose dependent studies (1). Control and treated cells were scrapped in 0.3mL of 2X SDS buffer (2% SDS, 100mM NaCl and 20mM Tris, pH 7.7) and cell lysates sonicated with Thermo Fisher Scientific 550 Sonic Dismembrator, prior to gel electrophoresis and Western blot analysis.

- **Cell live imaging using MitoTracker under Laser Confocal Microscopy**

ZR-75-1 cells treated with PRODH inhibitors (5mM 5-oxo and 5mM PPG) were harvested at 24, 48 and 72 hours of cell culture treatment on glass bottom microwell dishes MatTek Corporation (P35G-1.5-14-C) in RPMI media. 2.5µL of MitoTracker® Green FM Molecular Probes (Cell Signaling Technology) on 2 mL of charcoal stripped media (Gibco, Thermo Fisher Scientific, Carlsbad, CA) were added to ZR-75-1 cells (30 minute incubation). NucBlue™ Live Stain Ready Probes™ reagent with DAPI (Invitrogen by Thermo Fisher Scientific) stained the nuclei of cells.

❖ **Gel Electrophoresis, Western analysis and Immunoassays with Antibodies**

Cell lysates ran on Novex™ NuPAGE™ 4-12% Bis-Tris Protein Gel (Invitrogen™ Carlsbad, CA) using molecular weight markers (Amersham Full-Range Rainbow™ Recombinant Protein (GE Healthcare, San Ramon, CA) and transferred to Immobilon® -P nitrocellulose membrane (MilliporeSigma, St. Louis, MO). The membrane was blocked with 4% non-fat dry milk in 1X TBST, incubated with primary antibody (PRODH mouse monoclonal, 1µL/mL) overnight and β-actin (1µL/mL) for two hours, washed three times with 1X TBST, incubated with goat anti-mouse IgG secondary antibody conjugated to horse radish peroxidase (HRP) (0.1µL/mL) for one hour, and washed three times with 1X TBST before developing it with SuperSignal® West Pico Stable Peroxide Solution and West Pico Luminol/Enhancer Solution (Thermo Scientific). Chemiluminescent signal was captured on film and developed with Konica SRX-101A Medical Film Processor (Konica Corporation, Taiwan). Images were analyzed using *ImageJ FIJI* software (US National Institutes of Health, Bethesda, MD) (32). Relative protein levels were calculated by subtracting the intensity of each band from the background intensity and compared to β-actin and α-tubulin total protein intensity.

❖ **Isolating mitochondrial from ZR-75-1 cells**

Human breast epithelial cell lines, malignant ZR-75-1, DU4475, MCF7 and non-malignant MCF10A, were expanded *in vitro* and suspended in DMEM or RPMI media supplemented with 5% fetal bovine serum. Cells were treated with 5mM of either PRODH inhibitor (5-oxo or PPG) for 24, 48 and 72 hours, and harvested for mitochondria isolation. ZR-75-1 cells cultured in RPMI medium (control and 5mM PPG treated) were scraped in 1.2mL mitochondria isolation buffer (250mM sucrose, 10mM

Tris-HCl pH 7.4, 0.1mM EGTA, and deionized water) and homogenized with 50 strokes of a Dounce homogenizer. Samples with loose nuclei checked on an Olympus ULWCD Phase Contrast Microscope Condenser (20X magnification) were transferred to Eppendorf tubes and centrifuged for 6 minutes at 3,500 revolutions per minute (RPM) to pellet nuclei. Supernatant was centrifuged for 10 minutes at 13,000 RPM to pellet mitochondria. Nuclear pellet was solubilized in 2X SDS lysis buffer [100 mM NaCl, 20 mM Tris pH 7.5, 2% (by weight) SDS, DEPC water] and sonicated before freezing. Mitochondrial pellet was resuspended in 30-50 µL mitochondria isolation buffer and kept on ice for further analysis.

❖ **Mitochondrial PRODH enzymatic assay**

Mitochondrial NADH levels were measured by fluorescence spectrometry as a function of substrate and inhibitor treatment. Following substrate addition (proline and/or malate) to mitochondrial reactions in a 96-well plate format incubated at 37°C, a 15 minute time course measurement of NADH fluorescence was implemented (Fig. 5). Rotenone inhibited Complex 1 of the electron transport chain, blocking NADH oxidation (conversion to NAD^+). 30µL of resuspended intact mitochondria mixed with 165µL of 4mg/mL rotenone (MilliporeSigma, St Louis, MO) in KHE buffer (120mM KCl, 3mM HEPES, 5mM KH_2PO_4 pH 7.2) (195µL final volume) was transferred to a 96-well plate. 5µL of 40mM proline and/or 40mM malate were added to alternating wells and levels of NADH accumulated per reaction were determined using the PHERAStar FS fluorescent plate reader (BMG LABTECH GmbH, Offenburg, Germany) as described in detail in Gonçalves *et al* (21). Two of the wells received 5µL of 5mM PPG in Diethyl pyrocarbonate (DEPC) water (GeneMate) immediately before adding substrates.

❖ **Fly treatment and study – testing PPG in *Drosophila melanogaster***

At 7 days of age, male Oregon Red flies (Fly Base, Oregon-R, Roseburg, OR) were starved for 2 hours to synchronize feeding. Flies were transferred to vials (20/vial) containing 500µL of 5% w/v sucrose in water ± 5mM PPG absorbed in Whatman filter paper. Activity levels and survival were monitored 2X daily, and geotaxis measured daily by tapping flies to the bottom of the vial to assess climbing assay (30). 100µL liquid standard fly food was supplemented daily. Experiments were also performed in *slgA* null mutant flies (16) that lack the PRODH enzyme.

❖ **Xenografted mouse treatment and study (include health assessment, tumor measurements, sacrifice and snap freezing of organs/tumors)**

The Office of Ethics and Compliance at UCSF approved the IACUC protocol (approval #AN142193-02A) for animal studies PTC1797 and PTC1854 entitled "*In Vivo* Evaluation of Experimental Anti-Cancer Therapeutics; UCSF Preclinical Therapeutics Core" performed at the UCSF Comprehensive Cancer Center's Preclinical Core Facility, San Francisco, California, by Core Director, and Benz group collaborator, Dr. Byron Hahn, MD, PhD. Detailed methodologic description of these experimental MCF-7 xenograft systems are provided in Scott *et al*., OncoTarget 2017 (33), a publication that reported on tumor ER expression and did not address or describe the effects of PPG administration, as being reported now.

From nude mouse xenograft studies PTC1797, implanted with MCF7-xenografts, we isolated kidney whole cell lysate and kidney mitochondria for PRODH protein analysis. Vehicle mice were given vehicle saline solution (naïve mouse 970 and vehicle mice labeled 971, 974, 975) vs. PPG 50mg/kg three times a day, every other day for nine days,

by oral gavage (mice labeled 965, 966, 967), intravenously (mice labeled 962, 925, 968) and intraperitoneally (mice labeled 963, 964, 969). Two to three hours after third treatment, mice were sacrificed and organs (lung and kidneys) harvested in liquid nitrogen. From nude mouse xenograft studies PTC1854, implanted with MCF7-xenografts, we isolated tumor whole cell lysate and tumor mitochondria for PRODH protein analysis. Mice were administered daily doses of 50mg/kg PPG for 9 consecutive days by oral gavage. The control tumor-bearing mouse (#3883) was gavaged with saline solution daily, and started out with a slightly larger tumor on study day 58. Two mice (#3840 and #3880) each received 50mg/kg of PPG via oral gavage daily beginning 4/14/16 (study day 58) for nine days, ending 4/22/16 (study day 66). Tumor sizes were monitored before excision**.** Both studies were conducted to evaluate PPG's bioavailability and animal tolerance.

❖ **Isolating mitochondria from mice experiment**

Mice kidneys and tumors were pulverized under liquid nitrogen using 0.6mL mitochondrial isolation buffer with mortar and pestle. Samples were transferred to sterile Eppendorf tubes with another 0.6mL of mitochondrial isolation buffer and pipetted up/down gently, then transferred to Wheaton™ Dounce Tissue Grinders (150 strokes applied). Homogeneous cell lysates were centrifuged for 6 minutes at 3,500 RPM to pellet the nuclei. Supernatant was centrifuged for 10 minutes at 13,000 RPM to pellet mitochondria and those resuspended gently in 30µL of mitochondrial isolation buffer.

❖ **Laser Confocal Imaging Protocol & Immunocytochemistry Assays**

Cells imaged using Zeiss LSM 780 confocal microscope (Zeiss, Dublin, CA) with constant temperature enclosure and CO_2 regulation using 63X oil magnification in all

experiments. ZR-75-1 cells plated in 4-well glass slides from Lab-Tek®II (MilliporeSigma, St. Louis, MO) were treated with either 5mM PPG or 5mM 5-oxo for 24-48 hours. Cells were crosslinked with 4% paraformaldehyde in PBS (VWR, Radnor, PA) and blocked with IGEPAL® CA-630 NP 40 (MilliporeSigma, St. Louis, MO) made 10% in DEPC water, mixed with 5% normal goat serum (Cell Signaling Technologies, Danvers, MA) in PBS. Next, cells probed with a variety of primary and secondary antibodies, and ProLong® Gold antifade reagent with DAPI (Molecular Probes by Life Technologies, Thermo Fisher Scientific, Carlsbad, CA) were imaged at 63X oil magnification. Bitplane Imaris Software (Oxford Instruments, Concord, MA) used for 3D or 4D reconstruction and analysis of fixed and functional imaging data.

Results

In Vitro Study Results

Confocal microscopy used to examine the effects 5mM PPG treatment on ZR-75-1 cells for 24 hours and to evaluate the number of mitochondria and PRODH protein expression relative to other proteins, show a loss of PRODH protein intensity compared to vehicle treated cells (Fig. 7). Used as a marker for mitochondrial number, the intensity of TOM20, a protein located in the mitochondrial outer membrane remained unchanged throughout the experiment. The cytosolic enzyme Methylenetetrahydrofolate reductase (MTHFR) previously identified as a protein structurally similar to PRODH both in its structural organization and for containing a FAD moiety (13) remained unchanged throughout the experiment, while PRODH intensity was dramatically reduced (Fig. 8). The merged signal between MTHFR (cytoplasmic) and PRODH (mitochondrial) showed no overlap. Mouse monoclonal and rabbit polyclonal PRODH antibodies used produced similar results, discarding any possible antibody artifacts.

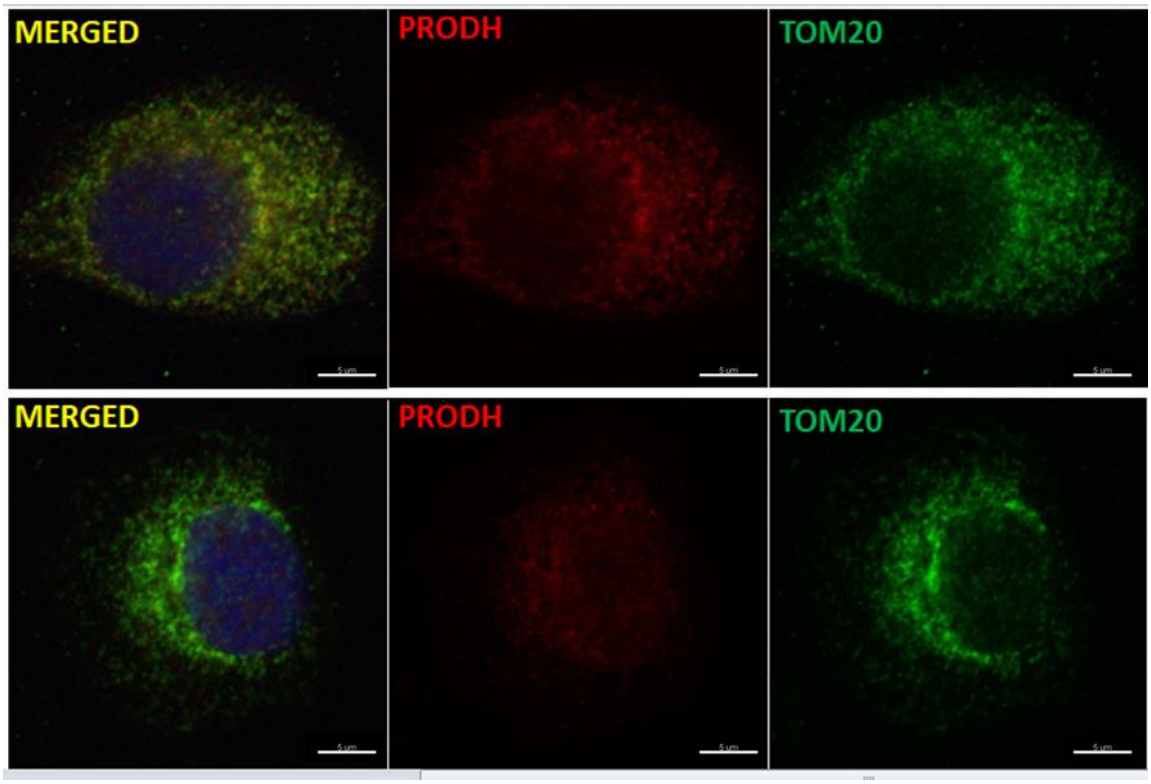

Figure 7. *Mitochondrial PRODH lost within 24h of PPG without mitochondrial destruction. PPG treatment induces early loss of mitochondrial PRODH protein before loss of outer mitochondrial membrane or later cell death.* Top panel untreated ZR-75-1 cells stained for PRODH (red) and mitochondrial TOM20 (green). Bottom panel identical to top panel but cells treated with 5 mM PPG for 24 hours.

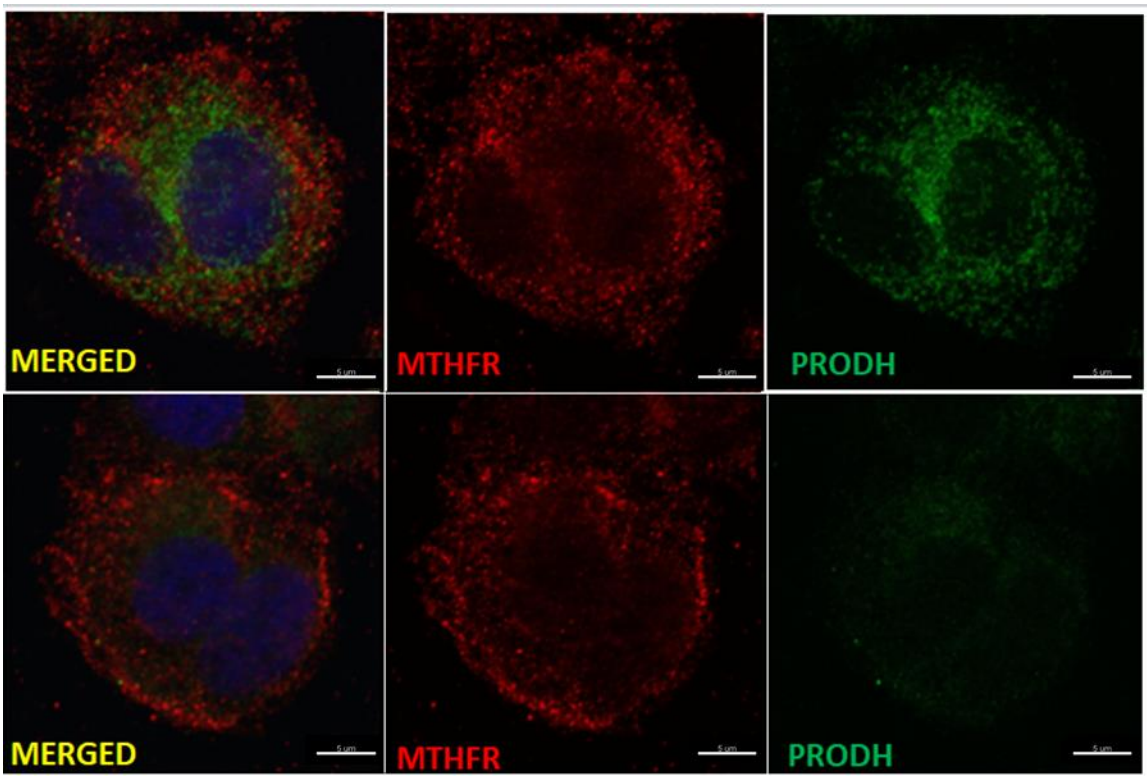

Figure 8. *Cytosolic MTHFR (FAD-containing) protein not affected by PPG validates western blot data.* Top panel untreated ZR-75-1 cells stained for cytosolic MTHFR (red) and PRODH (green). Bottom panel identical to top panel but cells treated with 5 mM PPG for 24 hours.

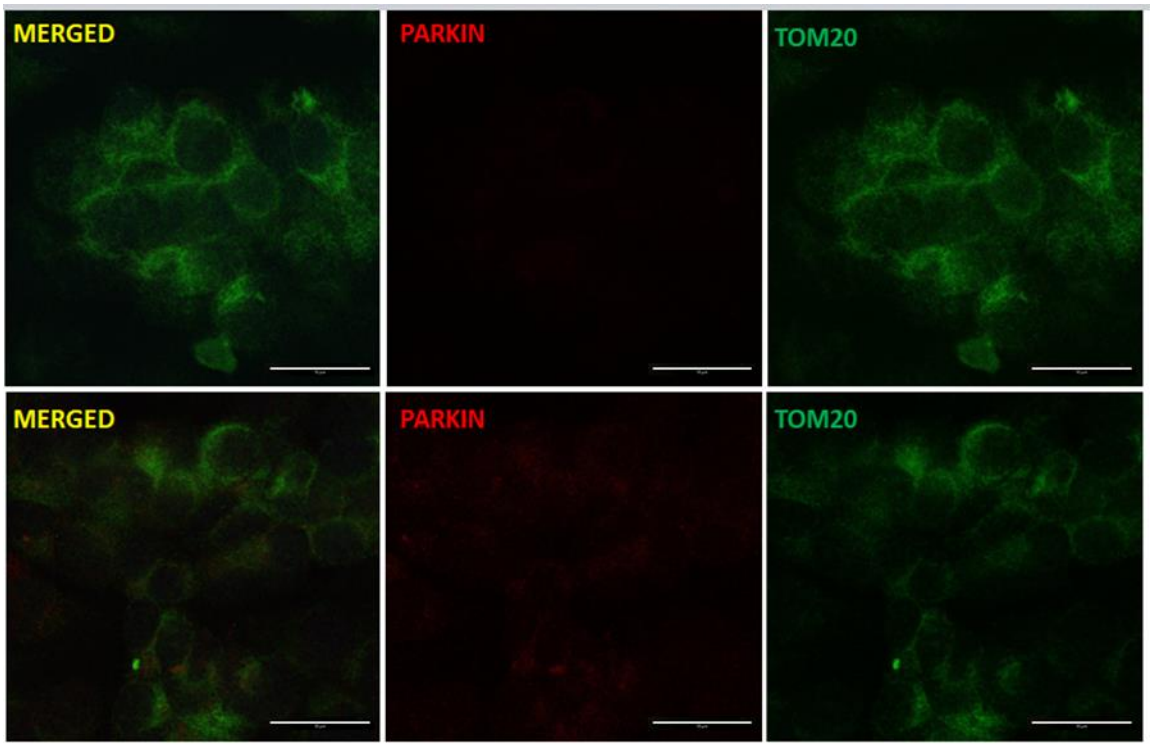

Figure 9A. *E3 ligase PARKIN not affected by PPG validates the absence of mitophagy.* Top panel untreated ZR-75-1 cells stained for Parkin (red) and mitochondrial TOM20 (green). Bottom panel identical to top panel but cells treated with 5 mM PPG for 24 hours.

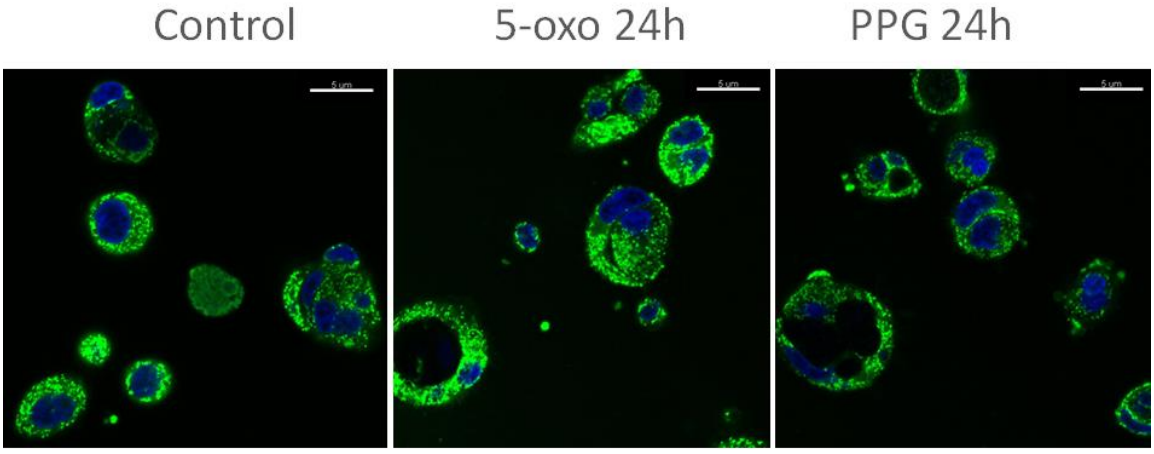

Figure 9B. *Live Cell Imaging of ZR-75-1 Cells*. Healthy mitochondria (green) detected after 24 hour treatment of 5-oxo and PPG using MitoTracker intercalating dye, a mitochondria marker. Comparable mitochondria marked in green punctate by MitoTracker shows no changes between treatments relative to control.

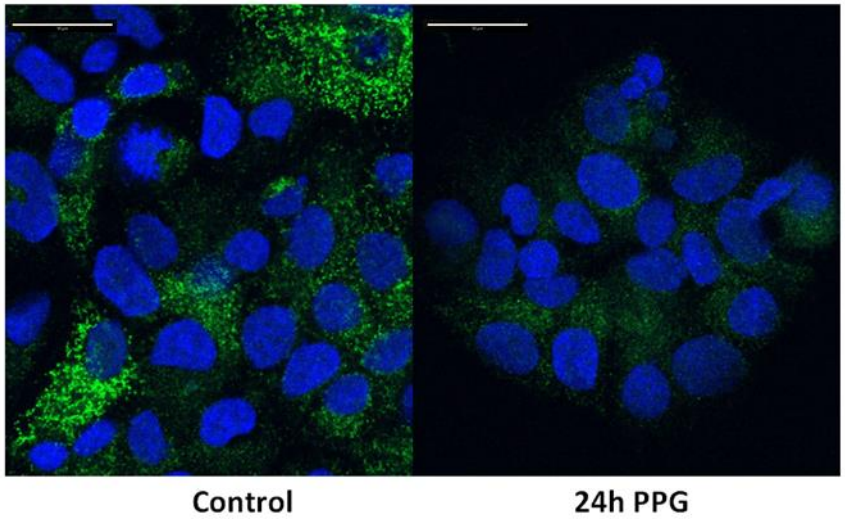

Figure 9C. *Laser confocal images of ZR-75-1 cells upon 24h PPG treatment displays PRODH (green) intensity diminished.* Compressed Z stack on confocal microscope of ZR-75-1 cells showing PRODH (green) intensity diminished on cells treated with 5mM PPG for 24 hours.

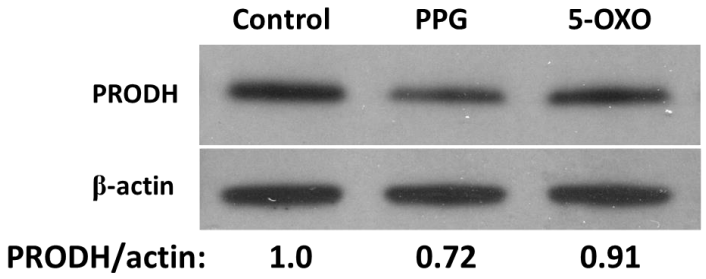

Figure 9D. *Western analysis and quantification of ZR-75-1 cells treated with 24h 5mM PPG versus 24h 5mM 5-oxo compared to vehicle control for their PRODH levels (67kD) normalized to β-actin (~40kD).* Western data confirms that 5-oxo has no significant impact upon PRODH levels. While PPG treatment (5mM) produces significant reduction in PRODH levels, 5-oxo (5mM) only slightly reduces PRODH levels.

The localization of PARKIN, an E3 ubiquitin ligase localized in the cytoplasm unless recruited to the mitochondria to initiate mitophagy, was analyzed upon 5mM PPG treatment of 24 hours. PARKIN'S distribution (red) within the cellular cytoplasm appeared augmented upon PPG treatment (Fig. 9A middle bottom panel); however its localization to the mitochondria was scarcely detected (Fig. 9A merged bottom panel). Live cell imaging using the mitochondrial specific intercalating fluorescent dye

MitoTracker confirmed that 5-oxo and PPG treatment of ZR-75-1 cells did not produce loss of mitochondrial number with similar mitochondrial fluorescence detected in control and treated samples (Fig. 9B). Additional confocal imaging (compressed Z stack) displayed PRODH (green) protein intensity diminished (Fig. 9C) while whole cell lysate from the same experiment confirms PPG produces significant reduction of PRODH levels relative to control and 5-oxo treatment (Fig. 9D). The PRODH competitive inhibitor 5-oxo shows no modelling effects on PRODH structure and does not induce PRODH protein decay (Fig. 9B, 9D).

Investigating UPR^{mt} activation by examining PPG influences on various mitochondrial stress signals

In search for markers of unfolded protein response, we examined GRP75, a 75 kDa Glucose-Regulated protein known to be part of the scaffold connecting the endoplasmic reticulum and mitochondria. Confocal microscopy was employed to evaluate the localization and interaction between GRP75 (red) and TOM20 (green). GRP75, extensively distributed in the mitochondria of control cells, is seen merged with TOM20 as a yellow signal (merged top panel); however its intensity is lost upon PPG treatment seen as mostly green in merged bottom panel (Fig. 10). Also examined as a marker of UPR^{mt}, HSP60 mitochondrial chaperone protein levels were upregulated 3-fold by PPG treatment relative to control and 5-oxo treated samples (Fig. 11).

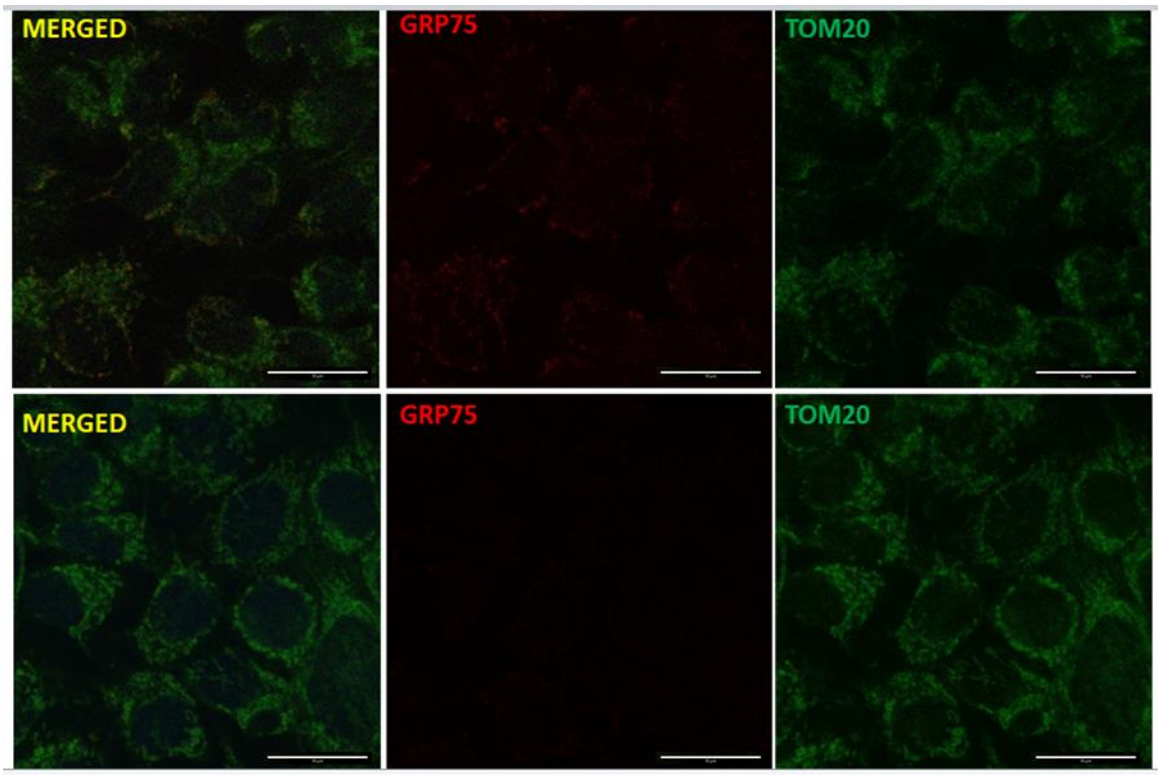

Figure 10. *GRP75 Communication with TOM20 in Mitochondria is disrupted after 24h PPG.* Top panel untreated ZR-75-1 cells stained for GRP75 (red) and mitochondrial TOM20 (green). Bottom panel identical to top panel but cells treated with 5 mM PPG for 24 hours.

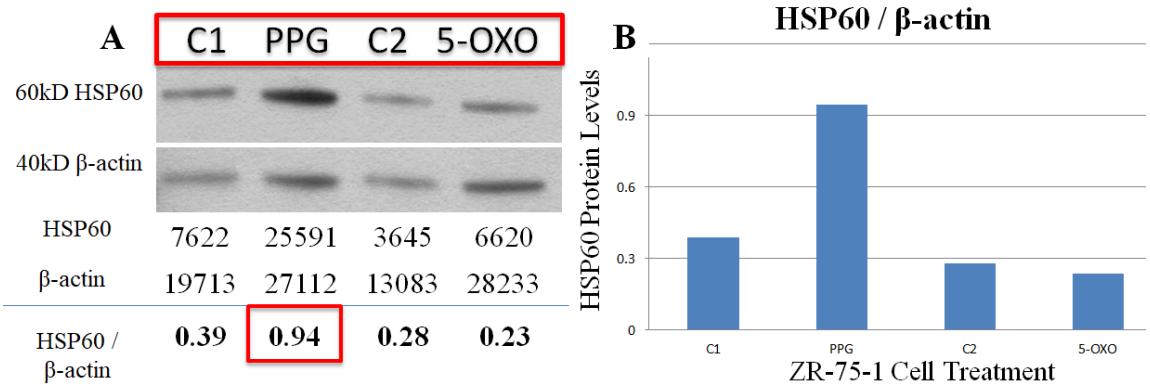

Figure 11. *ZR-75-1 cells treated with 24h PPG show elevated levels of HSP60.* (A) Western blot of ZR-75-1 whole cell lysate probed for HSP60 (60kD) and normalized to β-actin (~40kD) with C1/C2 control samples. (B) Bar graph quantifying normalized HSP60 values relative to β-actin.

Investigating PPG influences on mitochondrial protein PRODH through enzymatic assays

The accumulation of the downstream mitochondrial product, NADH, was measured in isolated mitochondria from ZR-75-1 cells (control and PPG treated), following addition of substrates (proline and malate). Cell treatment with 5mM PPG for 24 hours led to irreversible inhibition of mitochondrial PRODH with no NADH produced when proline was added (red line), while malate oxidation was not affected (Fig. 12). Rinsed mitochondria from above experiment showed same results. Control mitochondria (blue line) are capable of metabolizing proline and malate, seen as an increase in NADH levels.

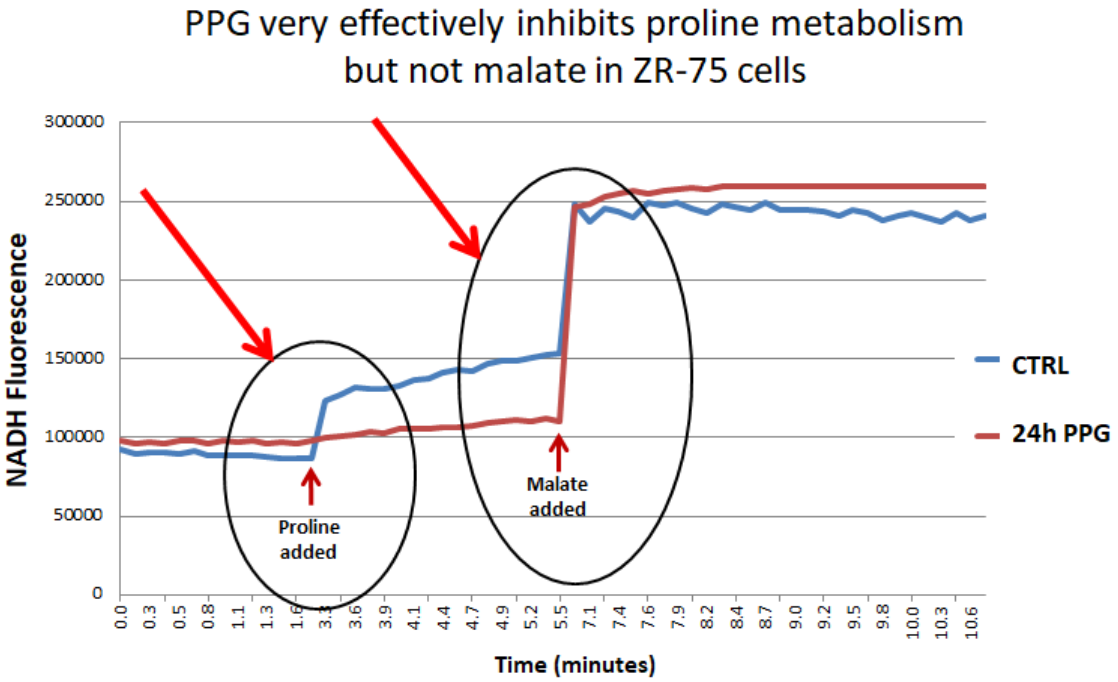

Figure 12. *ZR-75-1 cells vehicle and PPG treated given proline and malate to metabolize.* Graph displays NADH fluorescence measurements in vehicle (blue) and PPG treated (red) cells when proline and malate substrates are added to 96-well plate. Complex I of the electron transport chain is inhibited with Rotenone to prevent NADH oxidation.

In Vivo Study Results

The collaborative *Drosophila* study between the Benz and Jasper laboratories has shown induction of *Sluggish-A* phenotype following 48 h PPG oral administration to flies. Experiments detailed the *sluggish-A* null mutant flies and their phenotype (16). The clear viability of the treated flies exhibiting the identical phenotype as PRODH genetic knockout flies previously reported (16) represents our key rationale for undertaking the *in vivo* treatment of mice with PPG. As was shown in the video clip and discussed previously, the feeding of PPG to *Drosophila* flies mimics the "*Sluggish-A"* phenotype implying PPG's bioavailability and animal tolerance in millimolar concentrations without loss of viability or obvious adverse effects. Encouraged by these results in flies, preliminary studies using mice were undertaken to assess the consequences of *in vivo* PPG administration.

Nude mice experiments

Whole cell lysate and isolated mitochondria of kidneys of PPG-treated mice shows a reduction in PRODH protein levels relative to vehicle treated mice. It is noteworthy that potential tissue heterogeneity may account for differences in PRODH expression levels (Fig. 13, 14 and 15).

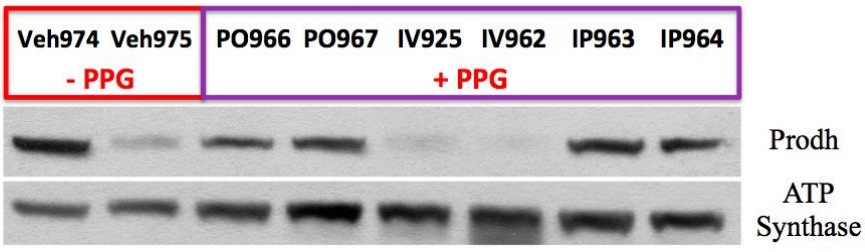

Prodh	21052	3233	9954	13914	1958	274	16498	11511
ATP synt	7955	8067	13377	19598	17504	18304	15352	13145
Prodh / ATP	2.65	0.40	0.74	0.71	0.11	0.01	1.07	0.88
synthase: (% +/- PPG)	100%	15.1%	27.9%	26.8%	4.2%	0.4%	40.4%	33.2%

Figure 13. *Western analysis of PRODH expression in whole cell lysate from mouse kidneys (+/- PPG treatment) shows PRODH level reduction in PPG treated vs vehicle.* Western blot showing whole cell lysate from frozen mouse kidneys (PTC1797); MCF7-xenografted nu/nu mice treated with vehicle (974, 975) vs. PPG 50 mg/kg x 3 (qod) in saline intravenously (IV925, IV962), intraperitoneally (IP963, IP964) and by oral gavage (PO966, PO967). Blot probed for PRODH (67kD) and normalizing mitochondrial protein ATP synthase (55kD).

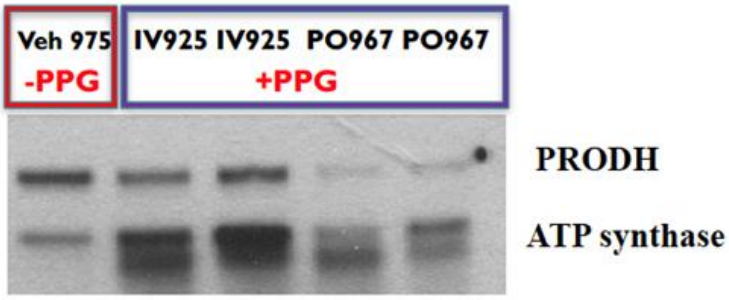

PRODH	21932	16270	21717	3557	8113
ATP synthase	7767	18729	26237	9812	13211
PRODH / ATP syn	2.82	0.87	0.83	0.36	0.61
(% +/- PPG)	100%	31%	29%	13%	22%

Figure 14. *Western analysis of PRODH expression in mitochondria isolated from mouse kidneys (+/- PPG treatments).* Western blot showing isolated mitochondrial from frozen mouse kidneys (PTC1797); MCF7-xenografted nu/nu mice treated with vehicle (975) vs. PPG 50 mg/kg x 3 (qod) in saline intravenously (IV925) and by oral gavage (PO967). Blot probed for PRODH (67kD) and normalizing mitochondrial protein ATP synthase (55kD).

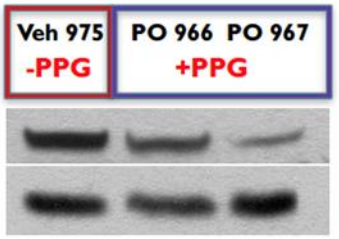

PRODH	53838	33939	11204
Cytochrome C	39097	34776	38528
PRODH / Cyto C	1.38	0.98	0.29
(% +/- PPG)	**100%**	**71%**	**21%**

Figure 15. *Western analysis showing isolated mitochondrial prepared from frozen mouse kidneys (PTC1797).* MCF7-xenografted nu/nu mice treated with vehicle (975) vs. PPG 50 mg/kg x 3 (qod) in saline by oral gavage (PO 966 and 967). Blot probed for PRODH (67kD) and normalizing mitochondrial protein Cytochrome C (15kD).

MCF-7 tumor xenograft study, PTC-1797

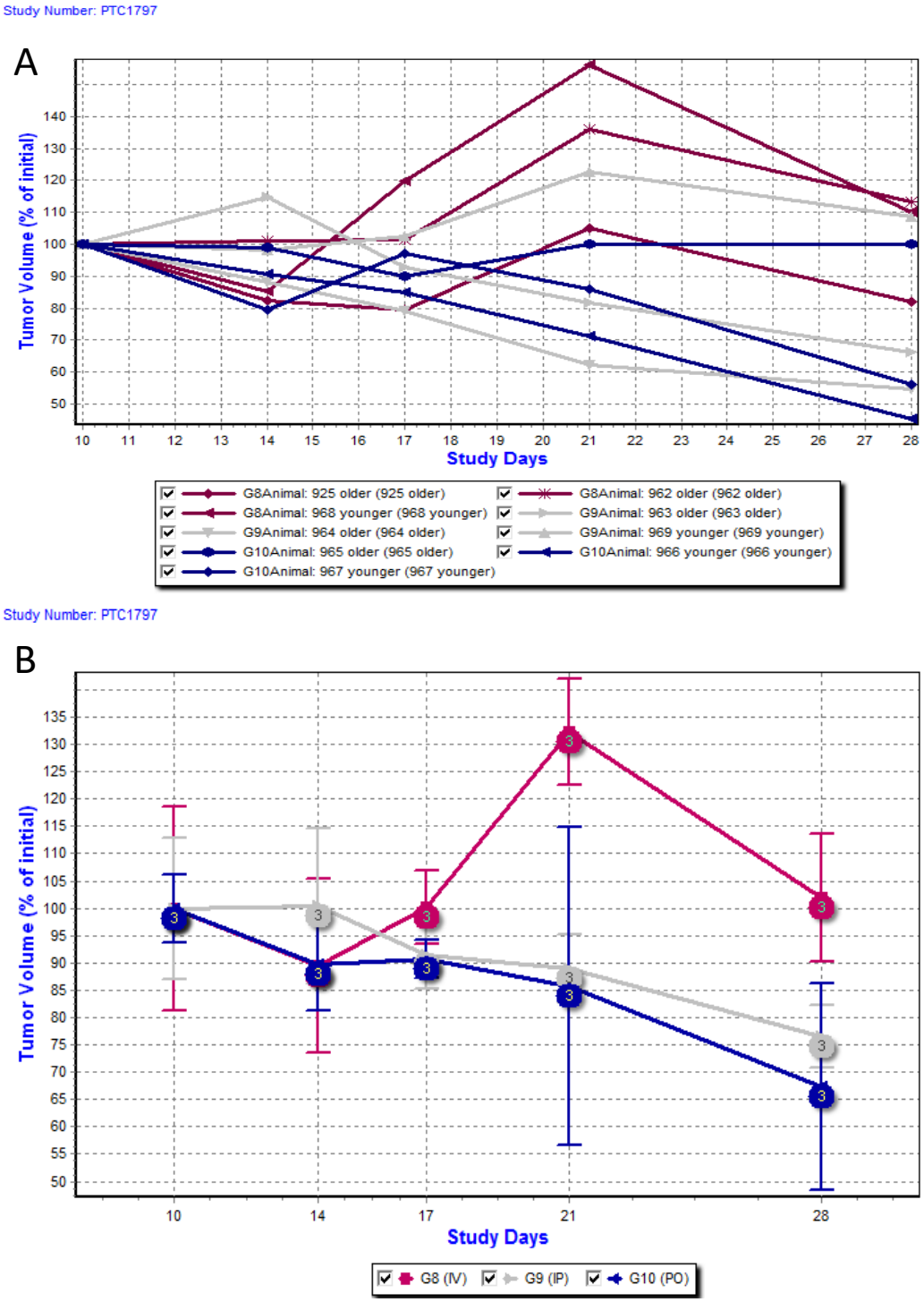

Figure 16. *PTC-1797 MCF7-xenografted nu/nu.* (A) Displays tumor volume measurements for nine mice (three per group PO, IV, IP) treated with PPG 50 mg/kg x 3 (qod); (B) Averages results per group (PO blue line, IV maroon line, IP gray line). Both display PPG treatment initiated at day 21 and PPG's ability to reduce tumor volumes (unpublished data).

Tumor volume (% of initial tumor volume) data collected on nine different MCF-7 tumor implanted (subcutaneously) mice, whose tumor volumes were tracked over time (Fig.16A). At day 10 after tumor implantation, tumor volumes were recorded as 100% and varying tumor volumes were tracked by different color lines (intravenously IV maroon lines; oral gavage PO blue lines; intraperitoneal IP gray lines). Mice drug treatment started at day 21 and every tumor showed volume reduction, except for that corresponding to mouse 965, who received PPG via oral gavage. Average tumor volume changes (also color coded) display the IV route of drug administration capable of 30% reduction in tumor volume, bringing it to the same size as day 10. IP route of drug administration showed a 25% reduction in tumor volume from day 10, and PO route of drug administration showed a 35% reduction, the most significant decrease in tumor volume indicating oral administered of PPG can reduce the volume of a subcutaneously implanted (xenografted) MCF-7 breast tumor (Fig. 16B).

MCF-7 tumor xenograft study, PTC-1854

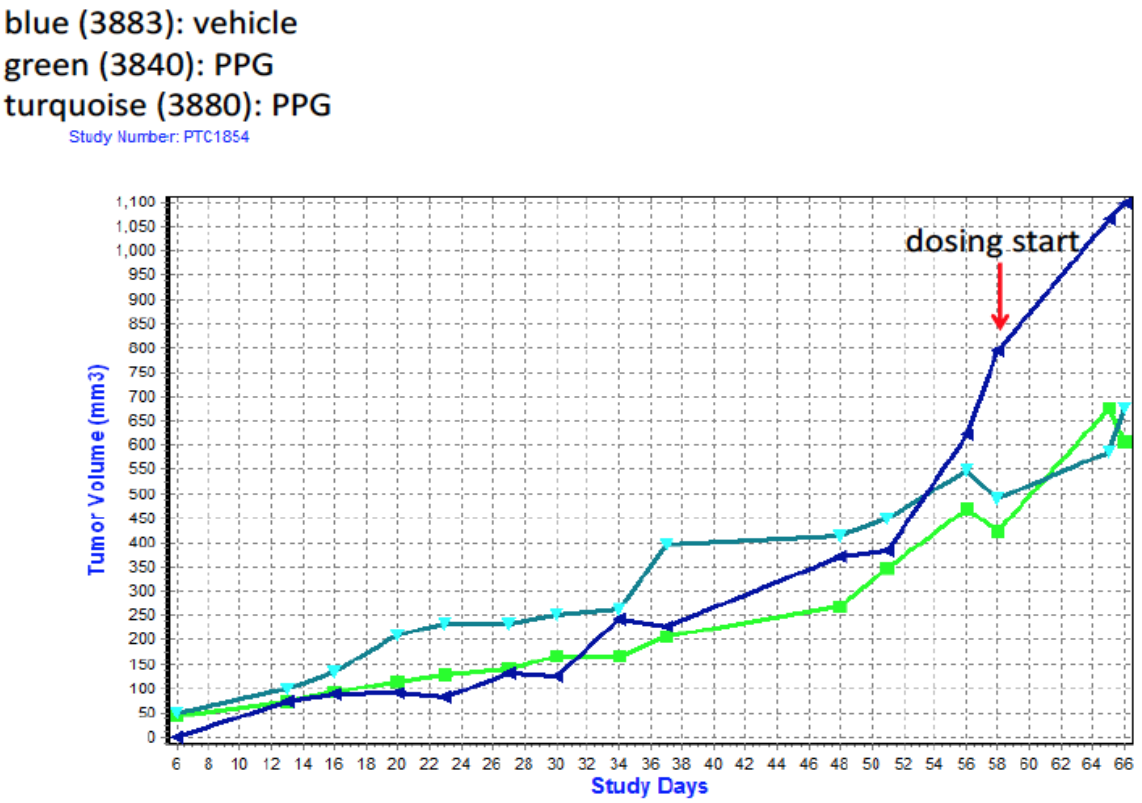

Figure 17. *PTC-1854 MCF7-xenografted nu/nu.* Graph displays tumor volume measurements for two mice treated with nine daily PO doses of PPG (50 mg/kg) – green (3840) and turquoise (3880) lines relative to control – blue (3883) line. Dosing started at study day 58 and mice were sacrificed at day 66 (unpublished data).

Similarly to PTC-1797, an identical strain of nude mice were implanted with a genetically modified clone of MCF-7 cells expressing a mutated (and constitutively active) form of ER that enables their tumorigenic growth in the absence of additional estradiol supplementation. These MCF/mutER xenografted mice were not treated shortly after implantation but only after well-established tumor growth (i.e. tumor volume >400 mm^3). At that time, mice were treated with nine daily doses of either vehicle (mouse 3883) or 50mg/kg of PPG (mice 3840 and 3880), via oral gavage, starting at day 58. All three mice tolerated their oral treatments well, showing no significant change in weight and continuously displaying healthy behaviors.

Tumor volume (% of initial tumor volume) data was collected until mouse sacrifice and tumor excision at day 66. While the control animal at this late stage of tumor growth showed exponential tumor growth after day 58, the PPG treated animals showed much more blunted growth after day 58, suggesting some PPG effect. However, when looking at the relative gain in tumor volume over the nine treatment days, both the PPG-treated and the vehicle control groups showed nearly 1.4-fold increases in tumor volume, indicating no significant antitumor effect of PPG on these well-established MCF-7 tumor xenografts (Fig. 17). While normal organs were not saved from this particular study, comparison of the three xenografted MCF-7/ERmut tumors isolated mitochondria showed reduced PRODH protein levels in PPG-treated mice (3880, 3840) relative to control (3883) (Fig 18). Lastly, using a goat anti-mouse light chain antibody helped eliminate problems with mouse heavy chain bands.

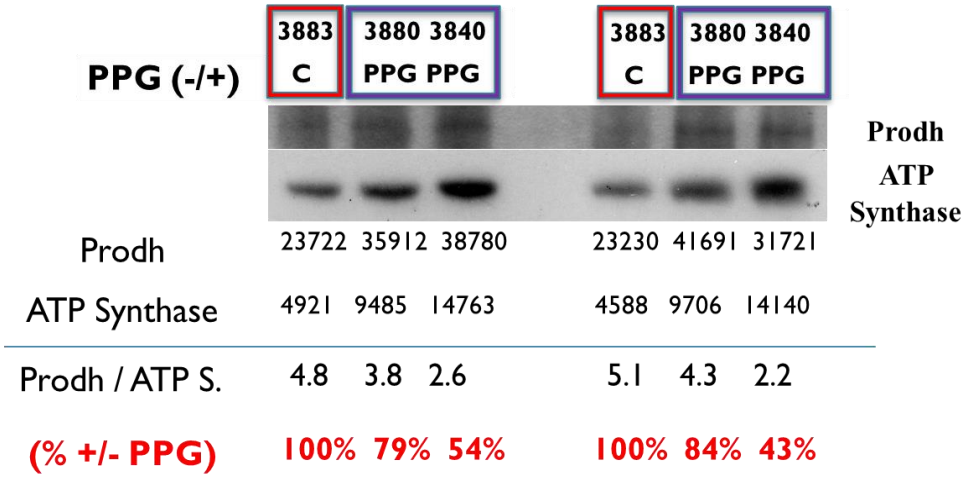

Figure 18. *Western Analysis of Isolated Mitochondria from frozen Mice Tumors (PTC1854) shows PRODH level reduction in PPG treated vs vehicle.* Western blot of technical replicates showing isolated mitochondrial prepared from frozen mouse tumors (PTC1854); MCF7-xenografted nu/nu mice treated with vehicle control (3883) vs. PPG 50 mg/kg x 9 daily doses in saline by oral gavage (3840, 3880). Blot probed for PRODH (67kD) and normalizing mitochondrial protein ATP synthase (55kD).

Discussion

The pursuit for PRODH inhibitors goes back nearly 40 years when this was considered a possible approach to eradicate tsetse flies and prevent African trypanosomiasis (34). The role of proline dehydrogenase (PRODH) in cancer progression has been previously explored *in vivo* (8, 19, 31) and the metabolism of proline by PRODH has been proposed to produce mitochondrial ROS and promote apoptosis in cancer cells (8, 21). However, former studies in the Benz laboratory provided evidence that PRODH can function to produce ATP, vital to cell survival, thus motivating our efforts to investigate PRODH inhibitors as cancer therapeutic agents. This project extends previous results targeting PRODH in various breast cancer cell lines by addressing both the mechanistic questions about mitochondrial stress induced by *in vitro* cell line treatments with the suicide PRODH inhibitor, PPG, as well as the *in vivo* feasibility of systemically administering PPG as a potential therapeutic. The use of confocal microscopy was essential to detect mitochondrial PRODH decay in ZR-75-1 breast cancer cells following PPG treatment without loss of mitochondria number (Fig. 7, 8, 9C). Additionally, using both confocal microscopy and Western analysis, these *in vitro* results are extended to demonstrate that PPG treatment promotes UPR^{mt} activation as assessed by cellular response of the stress proteins PARKIN, GRP75 and HSP60 (Fig. 9A, 10, 11). Finally, as a first step in addressing the potential bioavailability and *in vivo* effectiveness of PPG, results from mouse studies presented here support PPG as an effective biologic agent.

The use of immunocytochemistry analysis provided a new tool to examine the PRODH decay following PPG treatment (Fig. 7, 8). In all of these studies, TOM20

served as an excellent mitochondrial marker since it is a member of the TOM complex in the outer membrane of the mitochondria and responsible for recognizing and translocating mitochondrial proteins from the cytosol. TOM20 remained unchanged throughout PPG treatments, besides, without it the mitochondria would not survive. Initial *in vitro* results that PPG reduces PRODH protein intensity combined with mitochondrial assays (Fig. 5, 12) and structural modeling suggested PPG covalently modifies PRODH's FAD moiety causing pocket distortion (Fig. 4, 5, 6), which might be responsible for PRODH's disappearance within 24 hours (Fig. 6, 7, 8, 9C). Moreover, PPG was shown not to influence the levels of other mitochondrial proteins such as the complex-1 mitochondrial protein NDUFS1 (Fig. 6, 8) and complex-3 mitochondrial protein Rieske FeS [data not shown], as well as the extra-mitochondrial (cytosolic) FAD-containing protein methylenetetrahydrofolate reductase (MTHFR), structurally very similar to PRODH (Fig. 6, 8). It is noteworthy that two different PRODH antibodies were intentionally used, a mouse monoclonal and a rabbit polyclonal, with both antibodies producing similar results further validating these observations (Fig. 7, 8). Taken together, these results indicate PPG induces PRODH protein loss without loss of concurrent mitochondrial structures, while the similar TOM20 signal intensity between control and treated cells reveals that an equivalent number of mitochondria were present, proposing PPG does not induce loss of mitochondrial structures via mitophagy.

To investigate the possibility that PPG induces mitophagy, examination of PARKIN's localization (red) within the cellular cytoplasm appeared augmented upon PPG treatment possibly as PARKIN is recruited to the cytoplasm from the endoplasmic reticulum; however these results demonstrated little or no recruitment of PARKIN to the

mitochondria following PPG treatment, suggesting that mitophagy was not induced by PPG (Fig. 9A). As a caveat to this, Parkin-independent mitophagy scenarios have been reported (35) and in that regard cells may be undergoing mitophagy in a non-parkin dependent manner or on a time scale longer than the current experiments explored. In addition, it is also possible that if mitochondria are in fact being consumed by mitophagy, their synthesis compensates for this loss and explains our observation of no net change in TOM20 levels and intensity. Thus, using confocal microscopy to assess mitochondrial number, represented by TOM20 intensity, we determined that PPG induced no noticeable loss of mitochondrial number, while mitochondrial PRODH intensity was significantly diminished. Additionally, live cell imaging of cells treated with 5-oxo and PPG (Fig. 9B) shows similar mitochondrial fluorescence detected relative to control suggesting these PRODH inhibitors have no impact on mitochondrial number. Equally important, in response to mitochondrial stress, PARKIN binds to TOM20 in the mitochondrial outer membrane, and when activated, PARKIN adds ubiquitin chains to proteins to signal their mitochondrial degradation via the proteolytic pathway. Since PARKIN is not significantly affected by PPG treatment, that constitutes another piece of evidence consistent with absence of mitophagy, instead, arguing for activation of the mitochondrial unfolded protein response (UPR^{mt}) pathway resulting in PRODH degradation.

This activation of UPR^{mt} is a stress response initiated when misfolded proteins within the mitochondria overwhelm both its chaperone refolding and protein degrading capacities. In this regard, UPR^{mt} activation is a complex issue with the upregulation and coordination of many mitochondrial chaperone and proteases proteins such as HSP60 and Clp, respectively. As assessing UPR^{mt} activation by determining changes to these

proteins by confocal microscopy presented a technically challenging problem, examining the mitochondria's association with the membrane network of the endoplasmic reticulum was undertaken. Numerous studies have demonstrated that disruption of MAMs (mitochondrial associated membranes) occurs under conditions of mitochondrial stress and is also seen in many diseases such as cancers and Alzheimer's (36, 37). To examine PPG's capacity to promote the UPR^{mt}, we looked for evidence of alteration or disruption of the mitochondria's association with the endoplasmic reticulum (ER) using GRP75 as a marker. GRP75 is a scaffold protein anchoring MAMs to the mitochondria as they facilitate calcium homeostasis and fatty acid metabolism. Mainly a mitochondrial protein, GRP75 is also present in other organelles, and it has been reported to be disrupted under stress conditions, no longer making a communication bridge between ER and mitochondria (36, 37). In our control experiments, GRP75 co-localized with TOM20 in the mitochondria, but following PPG treatment, the intracellular distribution of GRP75 intensity was diminished relative to TOM20 (Fig. 10) suggesting loss of mitochondria homeostasis by induction of mitochondrial stress and likely activation of UPR^{mt}. To further validate the activation of UPR^{mt}, levels of the mitochondrial chaperone protein HSP60, another marker of mitochondrial stress, was investigated and shown to be upregulated following PPG treatment of breast cancer cells (Fig. 11A). While PPG induced a 3-fold increase in HSP60 levels compared to vehicle, the competitive inhibitor 5-oxo had essentially no influence upon HSP60 levels (Fig. 11B). Altogether, it appears that the covalent distortion of PRODH structure by the suicide inhibitor PPG is a novel effector of UPR^{mt} and our hypothesis that PPG induces structural distortions of PRODH and promotes a mitochondrial stress response (UPR^{mt}) is supported.

Next, working closely with our Buck Institute collaborator, Martin Brand, PhD, we have optimized our mitochondrial preparation technique and developed a bioassay capable of indirectly measuring inhibitor activity of mitochondrial PRODH by monitoring NADH levels upon substrate addition. While the known PRODH inhibitor L-THFA (at 5mM) produced approximately 70% reduction in proline's NADH generating capacity (27), and the 5-oxo competitive inhibitor identified by our modeling studies (Fig. 4A) produced a 95% reduction (at 5mM) in proline's NADH generating capacity, we compared those responses to that of the PRODH suicide inhibitor, N-propargylglycine (PPG). Our hypothesis that mitochondria isolated from PPG treated ZR-75-1 cells are unable to metabolize proline although able to metabolize malate was validated (Fig. 5, 12). In contrast, the effects of a competitive PRODH inhibitor, such as 5-oxo, are completely lost during the washout step. Thus, PPG treatment leads to immediate and irreversible loss of PRODH's enzymatic activity followed by its time-dependent selective degradation within the mitochondria of ZR-75-1 cells.

A crucial requirement for any cancer therapeutic is a drug's bioavailability and efficacy of action. In that regard, initial experiments with *Drosophila* flies shown in the video link demonstrate that feeding flies PPG at 5mM in sucrose solution recapitulated the "*Sluggish A*" phenotype characterized by PRODH knockdown or its genetic loss, and the inability to generate sufficient wing muscle ATP to power flight. Given the tolerability and bioavailability of orally administered PPG to flies, we extended our studies of PPG bioavailability and efficacy to mouse models. Kidney whole cell lysate and isolated kidney mitochondria from PPG-treated mice revealed lower PRODH protein levels relative to control (Fig. 11, 13, 14), consistent with our *in vitro* studies and *in vivo*

evidence in flies. PPG given orally (PO) to mice appeared optimally bioavailable and capable of inducing PRODH loss (Fig.14) when compared to other administration routes.

PPG treatment promotes *in vivo* loss of cellular PRODH in treated mice, particularly when assessed in intact isolated mitochondria that gives a stronger PRODH signal compared to the whole cell lysate, with ten times better results. Moreover, mitochondria isolated from frozen tumors excised from PPG-treated mice showed approximately one fifth of the PRODH levels detected in the tumor of control mice (Fig. 18). Even considering variability among animals, there is an apparent tumor volume reducing effect of PPG in these xenografted mice. Finally, as differential blood flows to organs versus xenografted tumors and heterogeneous levels of PRODH expression within different organ compartments may vary (kidney cortex vs. collecting system), variations were expected and observed between PRODH expression levels, and the effect of PPG on those, between independent preparations from the same frozen tissue material. Altogether, these results also led us to conclude that MCF-7 tumor xenografts are affected by PPG, but not particularly growth-limited by its administration *in vivo*, even though this cell line is known to be relatively insensitive to PRODH inhibitors due to low PRODH levels. Yet, the primary purpose of both these *in vivo* studies was to determine if systemically administered PPG could be detected in either the implanted tumor masses or normal mouse organs and we have revealed PRODH levels affected by PPG in both instances.

Reduction of the MCF-7 xenograft tumor volumes suggested that PPG not only reached at least a portion of the malignant cells resulting in decreased tumor PRODH levels (Fig. 18), but also produced detectable growth inhibiting effects of these cancers.

Such effects were most prominent when PPG was administered soon after tumor formation, while larger tumor masses seemed less affected suggesting limitations imposed by loss of vascular access. Recently, other investigators have begun exploring the *in vivo* potential of inhibiting PRODH expression in tumors, albeit using a less effective competitive PRODH inhibitor, L-THFA. Elia *et al* looked at tumors and metastases in 6-week old female BALB/c mice orthotopically inoculated with 4T1 or EMT6.5 mammary tumor cells. Primary breast tumors in their mouse models spontaneously produced metastases to the lungs in a short time with 100% penetrance. Primary tumors and body weight were monitored following PRODH inhibitor administration, without any observed adverse effects on healthy tissue and organ function (31). Their mouse studies, similarly to ours, showed minimal tumor volume changes in the large primary tumor implants but a significant reduction in the number of new lung metastases developed over the course of treatment. The employed 30mg/kg dose of L-THFA, relative to our 50mg/kg PPG doses, were given daily by intraperitoneal injections only, and no other administration route. Since the ultimate goal of such projects is to develop a drug therapy that might eventually be translated to human patients, it is vital to compare multiple routes of drug administrations, especially since intraperitoneal drug injection is not a typical or well accepted mode of anticancer drug administration in humans. Our project advances the field of cancer by comparing three different administration routes and testing multiple drug doses, concluding that oral and intravenous dosing are optimal for a drug candidate like PPG.

As a final point, cancer cell dependence on ATP production supports the development of therapeutic agents capable of targeting glutamate and ATP production,

thereby limiting the cancer's energy production and metabolic building blocks for macromolecular synthesis. Evidence presented here provides new mechanistic insight into PPG's role as a novel mitochondrially targeted anticancer agent with a unique mechanism of action, resulting in induction of mitochondrial stress and activation of the mitochondrial unfolded protein response (UPR^{mt}), depriving cells of PRODH by irreversibly inhibiting its enzymatic activity and also inducing its degradation.

Conclusions

This project's primary objectives were to address the mitochondrial consequences induced by the PRODH suicide inhibitor PPG, and the *in vivo* feasibility and bioavailability of administering PPG to live animals. These objectives were accomplished and our hypotheses validated. When reflecting on PPG's irreversible binding mechanism to PRODH, we have observed selective degradation of PRODH protein levels without loss of other mitochondrial proteins or mitochondria number, supporting a structural model and molecular mechanism of action in which PRODH distortion induces mitochondrial stress and activates its unfolded protein response, rather than mitophagy. In the worldwide search for new mitochondria-targeted cancer therapeutics, PPG offers a unique chemical tool to advance knowledge about mitochondrial biology as well as develop a new class of mitochondrial therapeutics.

When comparing the *in vivo* effects of PPG on normal kidneys and implanted tumors, our results provide evidence that PPG can be systemically administered by mouth and produce a pharmacodynamic effect at a distant mitochondrial site. Despite our need for an alternative PRODH expressing tumor model more sensitive to PRODH inhibition to conduct more extensive *in vivo* preclinical studies, we are confident our findings provide new and compelling rationale to pursue additional *in vivo* studies with our prototype PRODH suicide inhibitor, PPG.

PPG creates a non-hydrolysable bond within PRODH's catalytic site essentially preventing the entire subsequent cascade of events, including glutamate production vital for energy generation to fuel cancer cell survival. This complexed study touched upon many aspects of mitochondrial energetics and it provides a promising first step in the

investigation of PPG and its effects on cancer, hopefully helping countless people due to tumors' similarities across many cancer types.

References

1. Benz, C., Scott, G., (2014) Grant proposal: Targeting proline dehydrogenase (PRODH) induces synthetic lethal interactions with p53 restoring drugs and glutaminase (GLS1) inhibitors in breast cancer. A1 resubmission of grant proposal R21-CA187523 "Targeting proline metabolism produces a synthetic lethal interaction with p53 restoration."
2. Gary K. Scott, Justine Rutter, Katya Frazier, Daniel Rothschild, Christina Yau, Christopher Benz. A new anticancer strategy based on inhibiting mitochondrial proline dehydrogenase (PRODH) and exploiting synthetic lethal interactions with p53 restoration and/or glutaminase (GLS1) inhibition [abstract]. In: Proceedings of the 106th Annual Meeting of the American Association for Cancer Research; 2015 Apr 18-22; Philadelphia, PA. Philadelphia (PA): AACR; 2015. Abstract nr 5402
3. Andrea R. Daniel, Angela L. Gaviglio, Todd P. Knutson, Julie H. Ostrander, Douglas Yee, Carol A. Lange. Unliganded progesterone receptors augment estrogen-induced growth of breast cancer cells via co-regulation of estrogen receptor target genes [abstract]. In: Proceedings of the 104th Annual Meeting of the American Association for Cancer Research; 2013 Apr 6-10; Washington, DC. Philadelphia (PA): AACR; Cancer Res 2013; 73 (8 Suppl.): Abstract nr 3572. doi:10.1158/1538-7445.AM2013-3572
4. Manna, S., & Holz, M. K. (2016). Tamoxifen action in ER-negative breast cancer. Signal Transduction Insights, 5, 1-7. 10.4137/STI.S29901 [doi]
5. Neill, P., Martin Lesley-Ann, & Mitch, D. (2013). Biomarkers for the clinical management of breast cancer: International perspective. International Journal of

Cancer, 133(1), 1-13. 10.1002/ijc.27997 Retrieved from https://doi.org/10.1002/ijc.27997

6. Cheang, M. C., Voduc, D., Bajdik, C., Leung, S., McKinney, S., Chia, S. K., Nielsen, T. O. (2008). Basal-like breast cancer defined by five biomarkers has superior prognostic value than triple-negative phenotype. Clinical Cancer Research: An Official Journal of the American Association for Cancer Research, 14(5), 1368-1376. 10.1158/1078-0432.CCR-07-1658 [doi]
7. Sorlie, T., Perou, C. M., Tibshirani, R., Aas, T., Geisler, S., Johnsen, H., Borresen-Dale, A. L. (2001). Gene expression patterns of breast carcinomas distinguish tumor subclasses with clinical implications. Proceedings of the National Academy of Sciences of the United States of America, 98(19), 10869-10874. 10.1073/pnas.191367098 [doi]
8. Liu W, Phang JM. Proline dehydrogenase (oxidase), a mitochondrial tumor suppressor, and autophagy under the hypoxia microenvironment. Autophagy 8: 14071409, 2012.
9. Yoshida, G.J. Metabolic reprogramming: the emerging concept and associated therapeutic strategies. http://jeccr.biomedcentral.com/articles/10.1186/s13046-015-0221-y (2015)
10. Donald SP, Sun XY, Hu CA, Yu J, Mei JM, Valle D, Phang JM. Proline oxidase, encoded by p53-induced gene-6, catalyzes the generation of proline-dependent reactive oxygen species. Cancer Res. 2001 Mar 1; 61(5):1810-5.
11. Liu W, Le A, Hancock C, Lane A, Dang CV, Phang JM. Reprogramming of proline and glutamine metabolism contributes to the proliferative and metabolic responses regulated by oncogenic transcription factor c-MYC. Proc Natl Acad Sci USA 109:

8983-8988, 2012.

12. Servet C, Ghelis T, Richard L, Zilberstein A, Savoure A. Proline dehydrogenase: a key enzyme in controlling cellular homeostasis. Frontiers in Bioscience 17: 607-620, 2012.
13. Lee YH, Nadaraia S, Gu D, Becker DF, Tanner JJ. Structure of the proline dehydrogenase domain of the multifunctional PutA flavoprotein. Nat Struct Biol 10:109-114, 2003.
14. Liang, X., Zhang L., Natarajan SK., Becker DF. (2013, September 20). Proline Mechanisms of Stress Survival. Antioxidants & Redox Signaling, 19(9), 998-1011. doi:10.1089/ars.2012.5074
15. Neve RM, Chin K, Fridlyand J, *et al*. A collection of breast cancer cell lines for the study of functionally distinct cancer subtypes. Cancer Cell 10: 515-527, 2006.
16. Hayward, DC *et al.* "The *Sluggish-A* Gene of *Drosophila Melanogaster* Is Expressed in the Nervous System and Encodes Proline Oxidase, a Mitochondrial Enzyme Involved in Glutamate Biosynthesis." *Proceedings of the National Academy of Sciences of the United States of America* 90.7 (1993): 2979–2983. Print.
17. Polyak K, *et al*. A model for p53-induced apoptosis. Nature 389:300–305, 1997.
18. Pandhare J, Cooper SK, Donald SP, Phang JM. Regulation and function of proline oxidase under nutrient stress. J Cell Biochem 107: 759-768, 2009.
19. Phang JM, *et al*. The proline regulatory axis and cancer. Front Oncol 2: 60, 2012.
20. Liu W, Glunde K, Bhujwalla ZM, Raman V, Sharma A, Phang JM. Proline oxidase promotes tumor cell survival in hypoxic tumor microenvironments. Cancer Res 72: 36773686, 2012.
21. Gonçalves RL, Rothschild DE, Quinlan CL, Scott GK, Benz CC, Brand MD. Sources

of superoxide/H202 during mitochondrial proline oxidation. Redox Biology 2 (2014): 901-909.

22. Gary K. Scott, Beatrice C. Becker, Katya Frazier, Christina Yau, Christopher Benz. Targeting mitochondrial proline dehydrogenase (PRODH) with a mechanism-based irreversible inhibitor induces selective mitochondrial stress before cancer cell death [abstract]. In: Proceedings of the 107th Annual Meeting of the American Association for Cancer Research; 2017 Apr 1-5; Washington, DC. Philadelphia (PA): AACR; 2017. Abstract nr 1489
23. Rivlin, Noa *et al*. Mutations in the p53 Tumor Suppressor Gene: Important Milestones at the Various Steps of Tumorigenesis. Ed. Arnold J. Levine. Genes & Cancer 2.4 (2011): 466–474. PMC. Web. 13 Oct. 2016.
24. Benz, C. (2008). Impact of aging on the biology of breast cancer. Critical Reviews in Oncology/hematology, 66(1), 65–74. http://doi.org/10.1016/j.critrevonc.2007.09.001
25. Christina Yau, Bianca Gabriel, Gary Scott, Martin Brand, and Christopher C. Benz. Global metabolomics profiles distinguish malignant from non-malignant human mammary epithelial cell responses to endogenous p53 upregulation by MDM2 antagonism [abstract]. In: Proceedings of the 103rd Annual Meeting of the American Association for Cancer Research; 2012 Mar 31-Apr 4; Chicago, IL. Philadelphia (PA): AACR; Cancer Res 2012; 72 (8 Suppl.): Abstract nr 5160. doi:1538-7445.AM2012-5160.
26. Buck Institute for Research on Aging (2014). Inhibition of Proline Catabolism for the Treatment of Cancer and other Therapeutic Applications. U.S. Patent No. 62/079,382 filed Nov. 13, 2014. California: U.S.

27. T.A. White, N. Krishnan, D.F. Becker, J.J. Tanner. Structure and kinetics of monofunctional proline dehydrogenase from *Thermus thermophiles*. Journal of Biological Chemistry, 282 (2007), pp. 14316-14327, 10.1016/j.redox.2014.07.003 17344208

28. Yun, Jeanho *et al*. Mitohormesis. Cell Metabolism, Volume 19, Issue 5, 757 – 766.

29. Jensen MB, Jasper H. Mitochondrial proteostasis in the control of aging and longevity. Cell Metabolism. 2014; 20: 214-225. doi: 10.1016/j.cmet.2014.05.006.

30. Gargano JW, Martin I, Bhandari P, Grotewiel MS. Rapid iterative negative geotaxis (RING): a new method for assessing age-related locomotor decline in Drosophila. Exp Gerontol. 2005;40: 386-395. doi: S0531-5565(05)00034-3 [pii].

31. Elia, Ilaria *et al*. "Proline Metabolism Supports Metastasis Formation and Could Be Inhibited to Selectively Target Metastasizing Cancer Cells." *Nature Communications* 8 (2017): 15267. *PMC*. Web. 20 Oct. 2017.

32. Schindelin, J., *et al.* (2012), "Fiji: an open-source platform for biological-image analysis", *Nature methods* 9(7): 676-682, PMID 22743772, doi:10.1038/nmeth.2019, on Google Scholar. <http://www.nature.com/nmeth/journal/v9/n7/full/nmeth.2019.html>

33. Scott, GK., *et al*. "ERpS294 Is a Biomarker of Ligand or Mutational ERα Activation and a Breast Cancer Target for CDK2 Inhibition." *OncoTarget* 8.48 (2017): 83432–83445. *PMC*. Web. 11 Dec. 2017.

34. Tritsch D, Mawlawi H, Biellmann JF. Mechanism-based inhibition of proline dehydrogenase by proline analogues. Biochim Biophys Acta 1202: 77-81, 1993

35. Villa, Elodie *et al*., Parkin-Independent Mitophagy Controls Chemotherapeutic

Response in Cancer Cells. Cell Reports , Volume 20 , Issue 12 , 2846 – 2859

36. López-Crisosto, C., Bravo-Sagua, R., Rodriguez-Peña, M., Mera, C., Castro, P. F., Quest, A. F. G., Lavandero, S. (2015). ER-to-mitochondria miscommunication and metabolic diseases//doi.org/10.1016/j.bbadis.2015.07.011 Retrieved from http://www.sciencedirect.com/science/article/pii/S0925443915002033
37. Raturi, A., & Simmen, T. (2013). Where the endoplasmic reticulum and the mitochondrion tie the knot: The mitochondria-associated membrane (MAM)//doi.org/10.1016/j.bbamcr.2012.04.013 Retrieved from http://www.sciencedirect.com/science/article/pii/S0167488912001048
38. Bender H-U, Almashanu S, Steel G, Hu C-A. Functional Consequences of PRODH Missense Mutations. Am J Hum Genet 76: 409– 420, 2005.
39. Benz, C., Jasper, H., (2011) Calico Project proposal submitted: Targeting Proline Catabolism to Activate the UPR^{mt} Response as a Cancer-Aging Intervention
40. B.A. Baban, M.P. Vinod, J.J. Tanner, D.F. Becker. Probing a hydrogen bond pair and the FAD redox properties in the proline dehydrogenase domain of *Escherichia coli* PutA Biochimica et Biophysica Acta, 1701 (2004), pp. 49-59, 10.1016/j.redox.2014.07.003 15450175
41. Hargrove JW. Amino acid metabolism during flight in tsetse flies. J Insect Physiol 22:309-313, 1976.
42. Naser, A. Anjum (2014). Plant Adaptation to Environmental Change: Significance of Amino Acids and their Derivatives (Pages 70-71). Boston, MA: CAB International.
43. Christina Yau, Rachel Puckett, Akos A. Gerencser, Martin D. Brand, and Christopher C. Benz. Wildtype p53 upregulation induces contrasting bioenergetics and metabolic

responses in malignant and nonmalignant mammary epithelial cells [abstract]. In: Proceedings of the 102nd Annual Meeting of the American Association for Cancer Research; 2011 Apr 2-6; Orlando, FL. Philadelphia (PA): AACR; Cancer Res 2011; 71 (8 Suppl.): Abstract nr 3797. doi:10.1158/1538-7445.AM2011-3797

44. P.Y. Scaraffia, M.A. Wells. Proline can be utilized as an energy substrate during flight of *Aedes aegypti* females. Journal of Insect Physiology, 49 (2003), pp. 591-601, 10.1016/j.redox.2014.07.003 12804719
45. M.A. Moxley, J.J. Tanner, D.F. Becker. Steady-state kinetic mechanism of the proline: ubiquinone oxidoreductase activity of proline utilization A (PutA) from Escherichia coli. Archives of Biochemistry and Biophysics, 516 (2011), pp. 113-120, 10.1016/j.redox.2014.07.003 22040654
46. N. Krishnan, D.F. Becker. Oxygen reactivity of PutA from Helicobacter species and proline-linked oxidative stress. Journal of Bacteriology, 188 (2006), pp. 1227-1235, 10.1016/j.redox.2014.07.003 16452403
47. Wei Liu and James M. Phang (2013), CHAP Oncogene and Cancer - From Bench to Clinic: MiRNA and Proline Metabolism in Cancer, Dr. Yahwardiah Siregar (Ed.), InTech, DOI: 10.5772/55139. Available from: https://mts.intechopen.com/books/oncogene-and-cancer-from-bench-to-clinic/mirna-and-proline-metabolism-in-cancer